



Boundary layer control as a method of gas turbine blade cooling

Title	Boundary layer control as a method of gas turbine blade cooling
Item Type	Thesis
Authors	Ness, Dwight Osten
URI	https://hdl.handle.net/10945/6336
Publisher	University of Minnesota
Date Issued	1949-08
Download date	2026-04-14 05:02:16
Link to Item	https://hdl.handle.net/10945/6336

Downloaded from NPS Archive: Calhoun

Thesis
N4

Thesis
N4

Library
U. S. Naval Postgraduate School
Annapolis, Md.

BOUNDARY LAYER CONTROL AS A METHOD
OF GAS TURBINE BLADE COOLING

A THESIS

Submitted to the Graduate Faculty
of the
University of Minnesota

by
DWIGHT C. ^{Ten}NESS
COMDR. U.S.N.

In Partial Fulfillment of the Requirements
for the
Degree of Master of Science
in
Aeronautical Engineering

August

1949

CHAPTER I IN THE HISTORY OF THE
COURT OF THE COMMONS

CHAPTER I

CHAPTER I IN THE HISTORY OF THE
COURT OF THE COMMONS

CHAPTER I
IN THE HISTORY OF THE
COURT OF THE COMMONS

CHAPTER I IN THE HISTORY OF THE
COURT OF THE COMMONS

ACKNOWLEDGMENTS

The author wishes to express his sincere appreciation to the following who aided in this study:

Professors B. J. Robertson, W. A. Hall, T. M. Murphy, and K. E. Neuseier of the Mechanical Engineering Department, for their assistance, advice and suggestions.

Shop personnel of the Oak Street Laboratory for their assistance in construction of the test equipment.

APPENDIX

The other three to seven are listed below
also to the following and also in this study
Professor S. S. Roberts, R. S. Hall, L. S.
Kemp, and E. S. Bennett of the National Engineering
Department, for their assistance, advice and suggestions.
The personnel of the Oak Ridge Laboratory for
their assistance in maintenance of the test equipment.

TABLE OF CONTENTS

	Page
Title Page	
Acknowledgements	
Table of Contents	
Index of Tables and Figures	
Object and Scope	
Introduction	1
Test Equipment	6
Test Procedure	10
Test Results	11
Conclusions	14
Appendix	
Nomenclature	36
Bibliography and References	37
Sample Calculations	38

TABLE OF CONTENTS

Page

	1817-1818
	Administrative
	Table of Contents
	Index of Tables and Figures
	Notes and References
1	Introduction
8	Field Equipment
30	Field Procedures
41	Field Results
44	Discussion
	Appendix
58	Summary
62	Bibliography and References
66	Index of Tables and Figures

INDEX OF TABLES AND FIGURES

TABLES

Table		Page
I	Observed Test Data, Runs 1 and 2	15
II	Observed Test Data, Runs 3 and 4	16

FIGURES

Figures

1	Turboprop Engine Performance	17
2	Hollow Blade Cooling Effectiveness	18
3	Water Cooling Effectiveness	19
4	Rim Cooling Effectiveness	20
5	Ceramic Coating Effectiveness	21
6	Schematic of Test Layout	22
7	Test Section Mounted on Burner	23
8	Allison Engine	24
9	Control Panel	25
10	Cooling Air Meter	26
11	Test Blade (Conf. A)	27
12	Test Blade (Conf. B)	28
13	Test Section	29
14	Mounted Test Blade	30
15	End View of Blades	31
16	Graph (Conf. A)	32
17	Graph (Conf. A)	33
18	Graph (Conf. B)	34
19	Graph (Conf. B)	35

TABLES

Page	Title	Page
15	Summary Test Data, Runs 1 and 2	1
18	Summary Test Data, Runs 3 and 4	11

FIGURES

Page	Title	Page
17	Temperature versus Performance	1
18	Efficiency versus Cooling Efficiency	8
18	Water Cooling Efficiency	2
20	Air Cooling Efficiency	4
21	Temperature versus Cooling Efficiency	6
22	Summary of Test Layout	6
23	Test Section Mounted on Tower	7
24	Altitude Station	8
25	Control Panel	9
26	Cooling Air Water	10
27	Test Data (Cont. 1)	11
28	Test Data (Cont. 2)	12
29	Test Section	13
30	Mounted Test Unit	14
31	Test Flow of Water	15
32	Graph (Cont. 1)	16
33	Graph (Cont. 2)	17
34	Graph (Cont. 3)	18
35	Graph (Cont. 4)	19

OBJECT AND SCOPE

The object of this thesis was to determine the feasibility of cooling gas turbine blades by introduction of a controlled boundary layer of cool air over the blade surface.

This investigation included a static test of a single instrumented turbine blade in a variable high velocity, high temperature gas stream with variable cooling air flow. Two configurations of the test blade were used to produce variation in boundary layer control.

1940-1941

The object of this study was to determine the feasibility of using gas turbine blades by introduction of a controlled boundary layer of air over the blade surface.

This investigation included a study of a single laminated turbine blade in a turbine flow velocity high speed apparatus and also the effect of inlet air flow. The investigation of the test blade was used to provide criteria in boundary layer control.

INTRODUCTION

Maximum effort in the development of gas turbines is being exerted to improve specific power output, to reduce specific fuel consumption and to increase reliability. The most promising field for the attainment of these objectives lies in increasing the turbine inlet temperature which is presently limited by permissible operating temperatures of blading materials. An investigation of the gas turbine thermodynamic cycle reveals the magnitude of improvement possible by increasing turbine operating temperatures. Such an investigation conducted by the NACA (Ref. 1) shows that for a given mass flow of working fluid the specific power output is proportional and the specific fuel consumption is inversely proportional to the inlet temperature. Fig. 1 illustrates this relation.

The increase of turbine inlet temperature, however, is limited by high temperature strength of blade materials. The development of high temperature metals is proceeding, but at a slow rate. How slowly metallurgical progress has been made is shown in Fig. 83 of Ref. 2. Allowable blade temperatures advanced from 1180° F. in 1935 to 1200° F. by 1940 and to 1385° F. by 1945. The rate of increase has been no greater since 1945.

Non-metallic materials such as ceramics have yet to demonstrate their adaptability to the rigorous service

INTRODUCTION

Business effort in the development of the business
 is being passed to various scientific groups, as well as
 specific fuel management and the business efficiency. The
 need for training leads for the attainment of these objectives
 lies in increasing the level of scientific studies in
 general, limited by particular special requirements of
 various systems, in the application of the gas turbine
 technology. This results in the nature of the investment
 possible by increasing further scientific knowledge, and
 an investigation conducted by the staff (see, 1) shows that
 for a given area of work, the need for specific power
 output is proportional to the specific fuel consumption. It
 is usually proportional to the total temperature. Fig. 1
 illustrates this relation.

The subject of turbine inlet temperature, however,
 is limited to the maximum amount of blade materials.
 The development of high temperature alloys is proceeding,
 but at a slow rate. The already established practice has
 been to use in the 500-600°C. class of blade
 materials around 1000°C. in 1950-60. The rate of increase has been
 1000 and to 1500°C. by 1960. The rate of increase has been
 no greater since 1960.

The scientific material used as a basis for the
 to determine their applicability to the present system

requirements of turbine blading. As a result the use of some method of cooling the gas turbine blading presents itself as the method of allowing higher gas temperatures with present materials.

Several methods of blade cooling have been proposed and evaluated. A discussion of these methods as related to this thesis follows.

Late model German turbojet engines such as the Jung OO4 employed hollow turbine blade cooled internally by means of air blown into the root and exhausted at the tip. 1650° F. turbine inlet temperature was used with 7% of compressor air output required to cool blades approximately 400° F.

The NACA has proposed (Ref. 1) an improvement to this method by inserting a core in the blade, leaving a small annular air passage. It was found that the heat transfer from blade to cooling air was principally in the boundary layer and adjacent cooling air so the insert permitted similar cooling with less air flow. Fig. 2 graphs the results of this improvement.

Another cooling method consists of circulating water through internal passages in the blade. This system of cooling has accomplished very large blade temperature reductions. German applications (Ref. 3) conducted by Dr. Schmidt permitted 850-920° F. blade temperatures with a gas temperature of 2200° F. Fig. 3 shows an NACA analytical

Investigation of engine blades. In a recent test it was noted that during the gas turbine starting process it was found that the blades were damaged as well as the method of allowing slight gas temperature rise during starting.

Several methods of blade cooling were tried and compared. A discussion of these methods is given in the following.

The first method investigated consisted of the use of air cooled inlet turbine blades cooled internally by means of air blown into the root and mounted at the tip. This method of cooling was used with the turbine during its operation in order to determine its effect on the turbine.

The first test reported (Ref. 1) on investment in this method of internal cooling in the blades, testing a small turbine air engine. It was found that the heat transfer from the air cooling air was practically in the boundary layer and adjacent cooling air in the duct was highly efficient cooling with less air flow. Fig. 2 shows the results of this experiment.

Another cooling method consists of streamlining the flow through internal passages in the blades. This system of cooling has been investigated very largely by investigators. Various experiments (Ref. 3) conducted by the author resulted in the following results with a gas turbine at 2000 r.p.m. Fig. 3 shows an example of this method.

investigation of water cooling which also gave considerable blade temperature reduction. It must be pointed out that while water cooling is very effective, the problems of handling the high temperature, high pressure water flow at high rates makes service application of this method difficult.

A modification of the foregoing system, known as rim cooling, has also been tried. Here water is circulated through the rotor rim so as to extract heat from the blade root. Less temperature reduction is obtained and the disadvantages of the water coolant system still exist. Fig. 4 shows rim cooling effectiveness. It can be seen from the figure that having a blade material of high thermal conductivity, K_M , is essential to this method.

All of the foregoing methods employ the same basic principle of cooling. They do not inhibit the heat transmission to the blade, but do increase the internal conductivity, or removal of heat, thereby affecting cooling. The proposal of this thesis is to substitute a boundary layer of cool air over the blade's surface in order to inhibit the heat transmission from the hot gases to the blade.

A coating of high temperature ceramic of low conductivity would embody this same principle. Fig. 5 shows the effectiveness of ceramic coatings of various thicknesses. While this is a very promising field insofar as temperature of operation is concerned, the inherent defects of brittle-

Investigation of water cooling which also gave satisfactory
 glass temperature reduction. It must be noted that
 while water cooling is very effective, the results of
 heating the high temperature, high pressure water from a
 high water source involve application of this water directly
 will.

A modification of the foregoing system, known as
 the cooling, has also been tried. Here water is circulated
 through the tower and is returned back from the glass
 tank. This temperature reduction is obtained and the dis-
 advantages of the water cooling system will be noted. It
 shows the cooling effectiveness. It was to be noted that
 there was a slight reduction of high pressure water-
 level, etc. is essential to this system.

All of the foregoing methods enjoy the same
 basic principle of operation. They do not require the heat
 transmission in the glass, but do require the internal
 conductivity, or transfer of heat, thereby affecting cooling.
 The purpose of this device is to establish a boundary
 layer of cool air over the glass's surface in order to re-
 duce the heat transmission from the hot glass to the fluid.
 A coating of high temperature material of low con-
 ductivity will reduce the heat transfer. All of these
 the effectiveness of various designs of various materials.
 While this is a very promising field, further investigation
 of operation is necessary, the present status of this

ness, thermal shock sensitivity and low tensile strength have obviated service use of ceramic covered blading.

If a region of low thermal conductivity can be interposed between the gas and the blade, then the objective of blade cooling could be accomplished. The natural boundary layer on the blade is such a region. However, the natural boundary layer forms at the temperatures of the gas. In this experiment the use of relatively cool air from the engine compressor is suggested to form a lower temperature boundary layer.

The justification of this idea is based on one of the fundamental laws of heat transfer, Faurier's equation for conduction (Ref. 4). (Experience has shown radiation effects to be secondary). Stated mathematically for steady state conduction:

$$q = KA \frac{dt}{dx}$$

where q = rate of heat transfer.

K = coefficient of thermal conductivity.

A = cross-sectional area of path.

$\frac{dt}{dx}$ = temperature gradient in direction of heat flow per unit distance.

This law shows that for a given configuration the rate of heat transfer from gas to blade may be made by reducing K and/or $\frac{dt}{dx}$.

K for air is reduced by reducing temperature.

This is shown mathematically from Luchens equation:

heat, thermal conductivity and low thermal capacity
have obtained results on of various porous bodies.

If a region of low thermal conductivity can be

interposed between the gas and the plates, then the objective
of plate cooling will be accomplished. The natural tendency

of air layer on the plate is such a region. However, the
natural boundary layer forms at the temperature of the gas.

In this experiment the use of relatively cool air from the
region compressor is suggested to form a layer boundary

boundary layer.

The condition of this case is based on the of

the fundamental law of heat transfer, boundary equation
for conduction (Eq. 4), (convection) and from radiation

attempts to be made. (Detailed mathematically for steady
state conditions)

$$q = h_c \Delta T$$

where q = rate of heat transfer.

h_c = coefficient of thermal conductivity.

ΔT = temperature difference.

h_c = temperature gradient in direction of heat
flow per unit distance.

This law gives that for a given configuration the
rate of heat transfer from gas to plate will be made by re-

$$q = h_c \Delta T$$

For air in contact by various temperatures.

This is shown mathematically from following equation

$$K = K_{32} \frac{492 + C}{T + C} \left(\frac{T}{492} \right)^{3/2}$$

where T = absolute temperature

C = constant (.0129 for air).

K_{32} = K at 32° F.

The temperature gradient from the boundary layer to blade, $\frac{dt}{dx}$, is reduced by the use of the cool air controlled boundary layer. In fact, the cool air boundary layer will at first be lower in temperature than the blade so that the blade will transfer heat to the boundary layer. However, the temperature gradient from the hot gas to the boundary layer would be increased so it would be rapidly heated. The optimum configuration might therefore require a series of bleeds from the blade so the average temperature of the layer along the blade would be minimized.

In the author's experience a controlled boundary layer has been successfully employed to cool a liquid rocket nozzle. In 1936 the author collaborated in the construction of a liquid rocket motor in which a boundary layer of coolant air bled into the nozzle enabled prolonged operation. The nozzle was of mild steel yet endured the very high temperature rocket exhaust gases better than any contemporary nozzles of superior materials.

$$h = \frac{1}{2} \left(\frac{1}{\rho} + \frac{1}{\rho'} \right) \frac{1}{\cos \theta}$$

where ρ = absolute density

ρ' = density of air

θ = angle

The refractive index of the medium is given by $n = \frac{c}{v}$, where c is the velocity of light in vacuum and v is the velocity of light in the medium. The refractive index of a medium is a function of the wavelength of light. The refractive index of a medium is also a function of the temperature and pressure of the medium. The refractive index of a medium is also a function of the density of the medium. The refractive index of a medium is also a function of the composition of the medium. The refractive index of a medium is also a function of the state of the medium. The refractive index of a medium is also a function of the direction of the light. The refractive index of a medium is also a function of the polarization of the light. The refractive index of a medium is also a function of the frequency of the light. The refractive index of a medium is also a function of the amplitude of the light. The refractive index of a medium is also a function of the phase of the light. The refractive index of a medium is also a function of the direction of the medium. The refractive index of a medium is also a function of the polarization of the medium. The refractive index of a medium is also a function of the frequency of the medium. The refractive index of a medium is also a function of the amplitude of the medium. The refractive index of a medium is also a function of the phase of the medium.

In the case of a medium, the refractive index is a function of the wavelength of light. The refractive index of a medium is also a function of the temperature and pressure of the medium. The refractive index of a medium is also a function of the density of the medium. The refractive index of a medium is also a function of the composition of the medium. The refractive index of a medium is also a function of the state of the medium. The refractive index of a medium is also a function of the direction of the light. The refractive index of a medium is also a function of the polarization of the light. The refractive index of a medium is also a function of the frequency of the light. The refractive index of a medium is also a function of the amplitude of the light. The refractive index of a medium is also a function of the phase of the light. The refractive index of a medium is also a function of the direction of the medium. The refractive index of a medium is also a function of the polarization of the medium. The refractive index of a medium is also a function of the frequency of the medium. The refractive index of a medium is also a function of the amplitude of the medium. The refractive index of a medium is also a function of the phase of the medium.

TEST EQUIPMENT

Fig. 5 shows the complete test equipment layout schematically. The test blade was mounted in a closed test section supplied with hot gas from a single J-33 combustion chamber. Fig. 6 is a photograph of the test section mounted on the burner. Air was supplied to the burner from the compressor of a naturally aspirated Allison V-1710 engine, Fig. 7. The quantity of gas flow was regulated by throttling the Allison engine while its temperature was controlled by burner fuel pressure. The temperature of the blade was measured by two thermocouples. All control and measurement was done from the control panel adjacent to the gas turbine test cell. Fig. 8 is a photograph of the control panel. The air which formed the controlled boundary layer was supplied from the laboratory air main at regulated pressure. The quantity of cooling air was measured in a standard design sharp edged orifice meter, shown in Fig. 9.

The test blade was manufactured from a solid Juno 004 turbine blade. Availability was the reason for selection of this blade. The "tinidur" type alloy (30% nickel, 14% chrome, 1.75% titanium, 12% carbon, balance, iron) possessed very difficult machining properties and low thermal conductivity. The blade roots were cut off flat for convenient mounting and the tip shortened by 3/4 inch

TEST RESULTS

Fig. 3 shows the complete test equipment layout essentially. The test glass was mounted in a closed test chamber. The test glass was supplied with a steady 4-50 cc/min flow of air. The air was supplied to the chamber from the compressor of a naturally aspirated piston 2-1/2 in. dia. The quantity of air flow was regulated by a valve in the air line which is controlled by means of a pressure transducer. The temperature of the glass was controlled by two thermocouples. All control and measuring circuits were connected to the control panel adjacent to the gas turbine test cell. Fig. 4 is a photograph of the control panel. The air which flows through the controlled boundary layer was supplied from the laboratory air main at regulated pressure. The quantity of cooling air was measured in a standard air flow meter which was water cooled, shown in Fig. 5.

The test glass was constructed from a single piece of borosilicate glass. Availability was the reason for selection of this glass. The "thin" type glass (the standard, 1/4 in. thick, is better, in strength, release, etc.) is not available. The glass was cut off the standard sheet and the top edge was ground by the manufacturer.

because of space limitations in the test section.

For the first test, configuration A was manufactured. In this blade the cooling air supply hole was drilled up the blade from root to 1/4 inch of tip through the thickest section. This hole was .20 inch in diameter. The air bleed holes (1/16 inch) were drilled from blade surfaces joining the supply hole. They were placed at a 45 degree angle with blade surface. There were six bleed holes to each surface. The exits were ground out with a fish tail countersink pattern to distribute the bleed air spanwise. A .15 inch hole was drilled up the leading edge for location of the thermocouple tip at midspan. The trailing edge was too thin to permit similar treatment so a 3/32 inch hole was drilled chordwise at midspan to snugly hold a thermocouple bead. The thermocouple was lead in in a stainless steel tube one inch downstream and bent 90 degrees and cemented in the trailing edge hole. Figs. 12, 13 and 14 show the thermocouple mounting. Fig. 10 shows the A blade between a standard blade and a shortened standard blade. The boundary layer is introduced at approximately the 30% chord point.

Configuration B blade is shown in Fig. 11. The boundary layer air supply was introduced through a .15 inch drilled passage 1/4 inch behind the leading edge. A 60 degree included angle slot was milled down the length of the leading edge and 3/32 inch bleed holes drilled joining the

because of minor irregularities in the last section.

For the first test, configuration 1 was used.

First, on this side the cooling air supply was

driven by the blower from east to west in the

the nearest section. This was done, as seen in

the air flow diagram (Fig. 1) were drilled

without joining the supply side. They were

in degree with the main surface. There were

holes in each surface. The holes were

the full complement of holes to distribute

equally. A 1/2 inch hole was drilled

for location of the thermocouple tip at

the hole was the hole in the hole

that hole was drilled in the hole

a thermocouple hole. The thermocouple

thermocouple hole was in the hole

from the hole in the hole

it was in the hole

the hole between a hole

the hole. The hole

was the hole

the hole

the hole

the hole

the hole

the hole

the hole

the hole

supply passage. In this design the cooling enters the slot opposed by stagnation pressure and flows out of the slot on both edges, forming the boundary layer.

The test section consisted of the blade mounting block shown in Fig. 13, and two side plates made of six inch channel. The bottom was closed with a 1/2 inch plate so that the hot gases which entered at the top were constrained to exhaust through the open side. The entrance and exit dimension are 3.5 x 4.5 inches. Fig. 12 pictures the complete test section. Fig. 14 shows another view of the blade mounting block. The test blade is centrally located with two parallel mounted standard blades to guide the flow.

Temperatures of the test blade were measured by 20 gauge chromel-alumel thermocouples which read on a Brown recorder. The small size thermocouples provided fast response and use of standard sillimanite insulations in the blade. The insulators were ground slightly in diameter for mounting in blade. The thermocouple tips were firmly seated in 3/32 inch holes for maximum sensitivity to blade temperatures. The trailing edge thermocouple bead was buried completely to insure it would sense blade, rather than gas temperatures.

Compensated lead wires connected the thermocouples to the selector switch for the recorder to eliminate errors in readings by variation in ambient temperature. The gas

supply passage. In this design the vertical surface of the
aperture by atmospheric pressure and lines out of the air in
both edges, forming the secondary layer.

The last section consisted of the blade mounting
which shows in Fig. 41, and the side plates out of air
last shown. The bottom was closed with a 1/2 inch plate
so that the hot gases were trapped at the top and out-
drained to exhaust through the open side. The exhaust
and out diameter was 2.0 x 4.0 inches. The 1/2 inch
the complete test section. The 1/2 inch section was of
the blade mounting block. The test blade is completely 1/2-
inch with the previous mounted standard blades to make the
flow.

The purpose of the test blade was covered by
the same theoretical considerations which were in a form
referred. The main side characteristics are listed in
specimen and are in standard elliptical locations in the
blade. The incidence was found slightly in diameter for
mounting in blade. The aerodynamic data were fairly good
in 1950 but were not entirely satisfactory in 1951.
Other. The trailing edge characteristics were not tested and
likely to have been in some blade, which was the

conclusion.
The aerodynamic data were covered in the aerodynamic
so the writer will be the reader in elliptical forms
in relation of relation to aerodynamic characteristics. The test

temperature entering the test section, T_4 , was measured by a radiation shielded chromel-alumel thermocouple.

TEST PROCEDURE

The temperature of the test blade was read with and without cooling air flow under exactly similar flow conditions. This technique permitted comparison of the two temperatures obtained to show the blade reduction due to cooling air alone.

The Allison engine was first started and its speed set to obtain the desired flow rate of burner air. The flow rate was measured by means of the pressure drop across the orifice in the compressor inlet duct.

Next, combustion was initiated in the burner with the spark and acetylene flare and fuel pressure adjusted until desired gas temperature obtained. When conditions stabilized temperatures and pressures were recorded. During runs with cooling air, the flow rate was varied in increments of 1/10 inch of water and temperature recorded when stabilized.

In order to investigate the cooling effects over a broad range of gas velocities three settings of the Allison engine were used to give low, medium and high gas flow rates. However, the low flow rate is not included in this report as it was unrealistically low compared with actual turbine operation. The flow rate was below minimum idling rate for a J-33 engine.

TEST PROCEDURE

The temperature of the test blade was read with
 and allowed cooling air flow under exactly similar flow
 conditions. This temperature provided comparison of the test
 temperatures obtained to show the blade resistance due to
 cooling air alone.

The initial engine was fixed started and the
 speed set to obtain the desired flow rate of burner air.
 The flow rate was measured by means of the pressure drop
 under the orifice in the compressor inlet duct.

Heat, combustion was obtained in the burner with
 the speed and cooling air flow and fuel pressure adjusted
 until desired gas temperature was obtained. The conditions
 established temperature and pressure were recorded. Dur-
 ing time with cooling air, the flow rate was varied in in-
 crements of 1/10 inch of water and temperature recorded
 when stabilized.

In order to investigate the cooling blade over
 a broad range of gas velocities three settings of the
 engine burner were used to give low, medium and high gas
 flow rates. However, the low flow rate is not included in
 this report as it was unobtainable for comparison with
 other turbine operation. The flow rate was raised slightly
 during tests for a high engine.

TEST RESULTS

The results of the experiment are contained in tables I and II and the graphs, Figs. 16 through 19. The graphs are plotted to show temperature reduction versus weight of cooling air flow.

These graphs are similar in shape and show that the reduction in blade temperature was approximately twice as great in the leading edge as the trailing edge. This is to be expected because of the increase in boundary layer temperature resulting from heat transmission from the gas. Also, the thinness of the blade section near the trailing edge offers more resistance to heat flow internally.

The graphs also show that the temperature reduction rate is greatest (the slope is maximum) at low cooling air rates. This is evidence that the boundary layer is established at low flow rates and is effective in reducing heat transfer. Beyond a flow rate of .2 lb./min. most of the graphs become straight line functions. This apparently results from thickening of the boundary layer and shows the insulating effect is proportional to the thickness. This effect conforms with Fourier's law. The cooling effectiveness, particularly at low flow rates, is greater with this method than the method of Fig. 2.

RESULTS

The results of the experiment are contained in Tables I and II and the graphs, Figs. 10 through 12. The graphs are plotted in such a manner that the weight of cooling air flow

is plotted against the temperature of the air entering the chamber. The temperature is shown logarithmically since the variation in the cooling rate at the trailing edge of the

is to be expected because of the increase in boundary layer temperature resulting from heat transmission from the gas. Also, the position of the flame front near the trailing edge of the nozzle is shown in Fig. 11.

The results also show that the temperature of the gas in the chamber (the slope of the curve) is constant for all cases. This is evidence that the boundary layer is established at the flow rate and is therefore in the

chamber. The results show that the temperature of the gas in the chamber is constant for all cases. This is evidence that the boundary layer is established at the flow rate and is therefore in the

chamber. The results show that the temperature of the gas in the chamber is constant for all cases. This is evidence that the boundary layer is established at the flow rate and is therefore in the

chamber. The results show that the temperature of the gas in the chamber is constant for all cases. This is evidence that the boundary layer is established at the flow rate and is therefore in the

To illustrate the cooling effectiveness consider the J-33 turbojet engine. Maximum cooling of 280 F. at 1600 F. gas temperature could be accomplished with only 2% of compressor air.

Configuration A produced more uniform results than those of configuration B, as can be seen by comparing Figs. 16 and 17 with 18 and 19. Configuration A curves plotted more parallel and gave results proportional to gas temperature, while configuration B curves intersect and are out of order with gas temperature increments. Configuration A probably gave more uniform boundary layer formation, since the flows were convergent rather than opposed. It was calculated that the stagnation point on the leading edge would fall in the milled slot so the cooling air would spill over both surfaces of the blade and form good boundary layers. From the non-uniform results at different flow rates stagnation point shifting may be indicated. Also, turbulence in the test section may have prevented uniform boundary layer formation and promoted mixing. It is believed that had the blade been manufactured with boundary layer control slots of the type used in airplane practice, such higher quality results would have been obtained. This type bleed was considered but discarded because of the machining problems, which would have required machining beyond shop capacity.

The illustration shows the cooling characteristics of the
 the 1-21 tapered angles. Various cooling of 100 F. at
 1000 F. gas temperature could be accomplished with only
 25 of surrounding air.

Consequently a pressure of 1000 F. would be
 this case of convection, it is not as easy to
 find. It is not as if the 10, 20, 30, 40, 50, 60, 70, 80, 90, 100, 110, 120, 130, 140, 150, 160, 170, 180, 190, 200, 210, 220, 230, 240, 250, 260, 270, 280, 290, 300, 310, 320, 330, 340, 350, 360, 370, 380, 390, 400, 410, 420, 430, 440, 450, 460, 470, 480, 490, 500, 510, 520, 530, 540, 550, 560, 570, 580, 590, 600, 610, 620, 630, 640, 650, 660, 670, 680, 690, 700, 710, 720, 730, 740, 750, 760, 770, 780, 790, 800, 810, 820, 830, 840, 850, 860, 870, 880, 890, 900, 910, 920, 930, 940, 950, 960, 970, 980, 990, 1000, 1010, 1020, 1030, 1040, 1050, 1060, 1070, 1080, 1090, 1100, 1110, 1120, 1130, 1140, 1150, 1160, 1170, 1180, 1190, 1200, 1210, 1220, 1230, 1240, 1250, 1260, 1270, 1280, 1290, 1300, 1310, 1320, 1330, 1340, 1350, 1360, 1370, 1380, 1390, 1400, 1410, 1420, 1430, 1440, 1450, 1460, 1470, 1480, 1490, 1500, 1510, 1520, 1530, 1540, 1550, 1560, 1570, 1580, 1590, 1600, 1610, 1620, 1630, 1640, 1650, 1660, 1670, 1680, 1690, 1700, 1710, 1720, 1730, 1740, 1750, 1760, 1770, 1780, 1790, 1800, 1810, 1820, 1830, 1840, 1850, 1860, 1870, 1880, 1890, 1900, 1910, 1920, 1930, 1940, 1950, 1960, 1970, 1980, 1990, 2000, 2010, 2020, 2030, 2040, 2050, 2060, 2070, 2080, 2090, 2100, 2110, 2120, 2130, 2140, 2150, 2160, 2170, 2180, 2190, 2200, 2210, 2220, 2230, 2240, 2250, 2260, 2270, 2280, 2290, 2300, 2310, 2320, 2330, 2340, 2350, 2360, 2370, 2380, 2390, 2400, 2410, 2420, 2430, 2440, 2450, 2460, 2470, 2480, 2490, 2500, 2510, 2520, 2530, 2540, 2550, 2560, 2570, 2580, 2590, 2600, 2610, 2620, 2630, 2640, 2650, 2660, 2670, 2680, 2690, 2700, 2710, 2720, 2730, 2740, 2750, 2760, 2770, 2780, 2790, 2800, 2810, 2820, 2830, 2840, 2850, 2860, 2870, 2880, 2890, 2900, 2910, 2920, 2930, 2940, 2950, 2960, 2970, 2980, 2990, 3000, 3010, 3020, 3030, 3040, 3050, 3060, 3070, 3080, 3090, 3100, 3110, 3120, 3130, 3140, 3150, 3160, 3170, 3180, 3190, 3200, 3210, 3220, 3230, 3240, 3250, 3260, 3270, 3280, 3290, 3300, 3310, 3320, 3330, 3340, 3350, 3360, 3370, 3380, 3390, 3400, 3410, 3420, 3430, 3440, 3450, 3460, 3470, 3480, 3490, 3500, 3510, 3520, 3530, 3540, 3550, 3560, 3570, 3580, 3590, 3600, 3610, 3620, 3630, 3640, 3650, 3660, 3670, 3680, 3690, 3700, 3710, 3720, 3730, 3740, 3750, 3760, 3770, 3780, 3790, 3800, 3810, 3820, 3830, 3840, 3850, 3860, 3870, 3880, 3890, 3900, 3910, 3920, 3930, 3940, 3950, 3960, 3970, 3980, 3990, 4000, 4010, 4020, 4030, 4040, 4050, 4060, 4070, 4080, 4090, 4100, 4110, 4120, 4130, 4140, 4150, 4160, 4170, 4180, 4190, 4200, 4210, 4220, 4230, 4240, 4250, 4260, 4270, 4280, 4290, 4300, 4310, 4320, 4330, 4340, 4350, 4360, 4370, 4380, 4390, 4400, 4410, 4420, 4430, 4440, 4450, 4460, 4470, 4480, 4490, 4500, 4510, 4520, 4530, 4540, 4550, 4560, 4570, 4580, 4590, 4600, 4610, 4620, 4630, 4640, 4650, 4660, 4670, 4680, 4690, 4700, 4710, 4720, 4730, 4740, 4750, 4760, 4770, 4780, 4790, 4800, 4810, 4820, 4830, 4840, 4850, 4860, 4870, 4880, 4890, 4900, 4910, 4920, 4930, 4940, 4950, 4960, 4970, 4980, 4990, 5000, 5010, 5020, 5030, 5040, 5050, 5060, 5070, 5080, 5090, 5100, 5110, 5120, 5130, 5140, 5150, 5160, 5170, 5180, 5190, 5200, 5210, 5220, 5230, 5240, 5250, 5260, 5270, 5280, 5290, 5300, 5310, 5320, 5330, 5340, 5350, 5360, 5370, 5380, 5390, 5400, 5410, 5420, 5430, 5440, 5450, 5460, 5470, 5480, 5490, 5500, 5510, 5520, 5530, 5540, 5550, 5560, 5570, 5580, 5590, 5600, 5610, 5620, 5630, 5640, 5650, 5660, 5670, 5680, 5690, 5700, 5710, 5720, 5730, 5740, 5750, 5760, 5770, 5780, 5790, 5800, 5810, 5820, 5830, 5840, 5850, 5860, 5870, 5880, 5890, 5900, 5910, 5920, 5930, 5940, 5950, 5960, 5970, 5980, 5990, 6000, 6010, 6020, 6030, 6040, 6050, 6060, 6070, 6080, 6090, 6100, 6110, 6120, 6130, 6140, 6150, 6160, 6170, 6180, 6190, 6200, 6210, 6220, 6230, 6240, 6250, 6260, 6270, 6280, 6290, 6300, 6310, 6320, 6330, 6340, 6350, 6360, 6370, 6380, 6390, 6400, 6410, 6420, 6430, 6440, 6450, 6460, 6470, 6480, 6490, 6500, 6510, 6520, 6530, 6540, 6550, 6560, 6570, 6580, 6590, 6600, 6610, 6620, 6630, 6640, 6650, 6660, 6670, 6680, 6690, 6700, 6710, 6720, 6730, 6740, 6750, 6760, 6770, 6780, 6790, 6800, 6810, 6820, 6830, 6840, 6850, 6860, 6870, 6880, 6890, 6900, 6910, 6920, 6930, 6940, 6950, 6960, 6970, 6980, 6990, 7000, 7010, 7020, 7030, 7040, 7050, 7060, 7070, 7080, 7090, 7100, 7110, 7120, 7130, 7140, 7150, 7160, 7170, 7180, 7190, 7200, 7210, 7220, 7230, 7240, 7250, 7260, 7270, 7280, 7290, 7300, 7310, 7320, 7330, 7340, 7350, 7360, 7370, 7380, 7390, 7400, 7410, 7420, 7430, 7440, 7450, 7460, 7470, 7480, 7490, 7500, 7510, 7520, 7530, 7540, 7550, 7560, 7570, 7580, 7590, 7600, 7610, 7620, 7630, 7640, 7650, 7660, 7670, 7680, 7690, 7700, 7710, 7720, 7730, 7740, 7750, 7760, 7770, 7780, 7790, 7800, 7810, 7820, 7830, 7840, 7850, 7860, 7870, 7880, 7890, 7900, 7910, 7920, 7930, 7940, 7950, 7960, 7970, 7980, 7990, 8000, 8010, 8020, 8030, 8040, 8050, 8060, 8070, 8080, 8090, 8100, 8110, 8120, 8130, 8140, 8150, 8160, 8170, 8180, 8190, 8200, 8210, 8220, 8230, 8240, 8250, 8260, 8270, 8280, 8290, 8300, 8310, 8320, 8330, 8340, 8350, 8360, 8370, 8380, 8390, 8400, 8410, 8420, 8430, 8440, 8450, 8460, 8470, 8480, 8490, 8500, 8510, 8520, 8530, 8540, 8550, 8560, 8570, 8580, 8590, 8600, 8610, 8620, 8630, 8640, 8650, 8660, 8670, 8680, 8690, 8700, 8710, 8720, 8730, 8740, 8750, 8760, 8770, 8780, 8790, 8800, 8810, 8820, 8830, 8840, 8850, 8860, 8870, 8880, 8890, 8900, 8910, 8920, 8930, 8940, 8950, 8960, 8970, 8980, 8990, 9000, 9010, 9020, 9030, 9040, 9050, 9060, 9070, 9080, 9090, 9100, 9110, 9120, 9130, 9140, 9150, 9160, 9170, 9180, 9190, 9200, 9210, 9220, 9230, 9240, 9250, 9260, 9270, 9280, 9290, 9300, 9310, 9320, 9330, 9340, 9350, 9360, 9370, 9380, 9390, 9400, 9410, 9420, 9430, 9440, 9450, 9460, 9470, 9480, 9490, 9500, 9510, 9520, 9530, 9540, 9550, 9560, 9570, 9580, 9590, 9600, 9610, 9620, 9630, 9640, 9650, 9660, 9670, 9680, 9690, 9700, 9710, 9720, 9730, 9740, 9750, 9760, 9770, 9780, 9790, 9800, 9810, 9820, 9830, 9840, 9850, 9860, 9870, 9880, 9890, 9900, 9910, 9920, 9930, 9940, 9950, 9960, 9970, 9980, 9990, 10000.

It is estimated that the maximum point on the leading
 edge will fall in the region of the cooling air
 would still over each surface of the blade and the heat
 boundary layers. From the measurements made at different
 the two maximum points which may be indicated.
 also, emphasis is to be made on the fact that the
 surface boundary layer formation and growth stage. It
 is believed that the blade heat transfer will depend
 on the angle of attack of the flow and in certain cases
 that, with slight quality results which have been obtained.
 This type of flow was considered and detailed account of the
 boundary conditions, which would have regular conditions in
 the flow field.

Uncontrollable variation in the speed of the Allison engine contributed to inaccuracy of data. A "hunting" of about fifty RPM occurred during much of the running, which produced 500 RPM variations in compressor speed. The variation in burner air flow caused drifting of gas temperatures.

Comparison of Figs. 16 with 17, and 18 with 19, shows cooling effectiveness variation with gas flow rate. Cooling effectiveness is greater at the lower flow rate. This is consistent with the laws of heat transmission by convection. The heat transfer from gas to blade increases with velocity.

From all graphs, the blade temperature reduction is shown to increase with gas temperature. This, also, is compatible with the laws of heat transfer, the $\frac{dt}{dx}$ term of Fourier's equation increases so more heat is transferred to the outer boundary layer. But, the heat transfer to the blade through the laminar sublayer is of such small magnitude that the net effect is greater blade temperature reduction.

temperature variation in the space of 200

feet. The variation in the space of 200

feet, which produced 1000 ft. variation in temperature

speed. The variation in temperature in the same distance

is the same.

Temperature of air, 10 ft. 19, and 10 ft. 20.

Temperature of air, 10 ft. 19, and 10 ft. 20.

Temperature of air, 10 ft. 19, and 10 ft. 20.

Temperature of air, 10 ft. 19, and 10 ft. 20.

Temperature of air, 10 ft. 19, and 10 ft. 20.

Temperature of air, 10 ft. 19, and 10 ft. 20.

Temperature of air, 10 ft. 19, and 10 ft. 20.

Temperature of air, 10 ft. 19, and 10 ft. 20.

Temperature of air, 10 ft. 19, and 10 ft. 20.

Temperature of air, 10 ft. 19, and 10 ft. 20.

Temperature of air, 10 ft. 19, and 10 ft. 20.

Temperature of air, 10 ft. 19, and 10 ft. 20.

Temperature of air, 10 ft. 19, and 10 ft. 20.

Temperature of air, 10 ft. 19, and 10 ft. 20.

Temperature of air, 10 ft. 19, and 10 ft. 20.

Temperature of air, 10 ft. 19, and 10 ft. 20.

Temperature of air, 10 ft. 19, and 10 ft. 20.

Temperature of air, 10 ft. 19, and 10 ft. 20.

Temperature of air, 10 ft. 19, and 10 ft. 20.

Temperature of air, 10 ft. 19, and 10 ft. 20.

Temperature of air, 10 ft. 19, and 10 ft. 20.

CONCLUSIONS

In view of the limited scope of the experimental tests, no detailed quantitative conclusions can be drawn. However, the results obtained from the foregoing tests do support the following general conclusions:

1. The introduction of a boundary layer of relatively cool air on a turbine blade in a high temperature, high velocity gas stream inhibits the transmission of heat from the gas to the blade, more than through the natural boundary layer, and results in reduction of blade temperature.

2. The magnitude of the reduction in blade temperature is proportional to the weight flow of air introduced into the boundary layer up to the limit investigated of 2% of the gas flow in an equivalent full scale engine.

3. This method of blade cooling is feasible insofar as weight flow of cooling air required to accomplish useful blade temperature reduction is concerned.

The results of the experiments are given in Table I.

DISCUSSION

In view of the limited scope of the experimental tests, no detailed quantitative discussion can be drawn. However, the results obtained from the foregoing tests do support the following general conclusions.

1. The introduction of a secondary layer of thin film on a turbine blade in a high temperature, high velocity gas stream results in the formation of a thin film on the blade, with this layer the normal secondary layer, and results in reduction of blade temperature.

2. The reduction of the reduction in blade temperature is proportional to the weight film of air film. Thus the secondary layer of the film investigated of all of the film in the experiments will minimize.

3. The nature of blade cooling is greatly influenced by the weight film of cooling air relative to secondary layer film temperature reduction in secondary.

TABLE I

OBSERVED TEST DATA

HIGH AIR FLOW RUNS
 COMPRESSOR RPM - 24,000
 — GAS TEMPS —

COOLING AIR ΔP "H ₂ O	W _a	800°F				1000°F				1200°F				1400°F				1600°F			
		TBLE	T.R.	TBLE	T.R.	TBLE	T.R.	TBLE	T.R.	TBLE	T.R.	TBLE	T.R.	TBLE	T.R.	TBLE	T.R.	TBLE	T.R.		
0	0	785		785		995		995		1190		1195		1390		1390		1585		1585	
.1	.217	720	65	760	25	920	75	965	30	1110	80	1150	45	1255	135	1325	65	1440	145	1615	70
.2	.345	710	75	755	30	920	75	965	30	1070	120	1135	60	1255	135	1325	65	1440	145	1595	80
.3	.471	700	85	750	35	895	100	950	45	1050	140	1135	60	1220	170	1310	80	1385	200	1480	105
.4	.600	690	95	735	50	875	120	945	50	1030	160	1110	85	1200	140	1300	90	1350	235	1465	120
.5	.726	675	110	730	55	855	140	937	58	1015	175	1115	80	1185	205	1290	100	1335	250	1450	135
.6	.846	665	120	730	55	850	145	930	65	1015	175	1115	80	1160	230	1270	100	1320	265	1450	135

RUN 1
 CONFIGURATION A
 RUN 2
 CONFIGURATION B

	800°F	1000°F	1200°F	1400°F	1600°F
P _f PSI	67	76	84	96	107
W _f lb/hr	74	93	107	129	146
ΔP _{B.A.} "Hg	1.83	1.82	1.80	1.65	1.50
W _{B.A.} lb/SEC	2.85	2.845	2.83	2.71	2.59
P ₃ "Hg	14.8	15.0	16.1	17.1	16.8
P _{E3} "Hg	15.4	15.4	16.5	17.5	17.2
P ₄ "Hg	.72	.64	.60	.52	.50
P _{E4} "Hg	11.45	11.8	13.1	13.75	13.8
g "Hg	10.63	11.16	12.5	13.23	13.3
M ₄	.731	.75	.795	.82	.823

TEMP: COOLING AIR - 80°F
 AMBIENT (T.CEL) 120°F

PRESS: ATMOS - 29.82 "Hg
 AMBIENT (TEST CELL) 27.50 "Hg

TABLE II

OBSERVED TEST DATA
 MEDIUM BURNER AIR FLOW RUNS
 COMPRESSOR RPM - 13,250

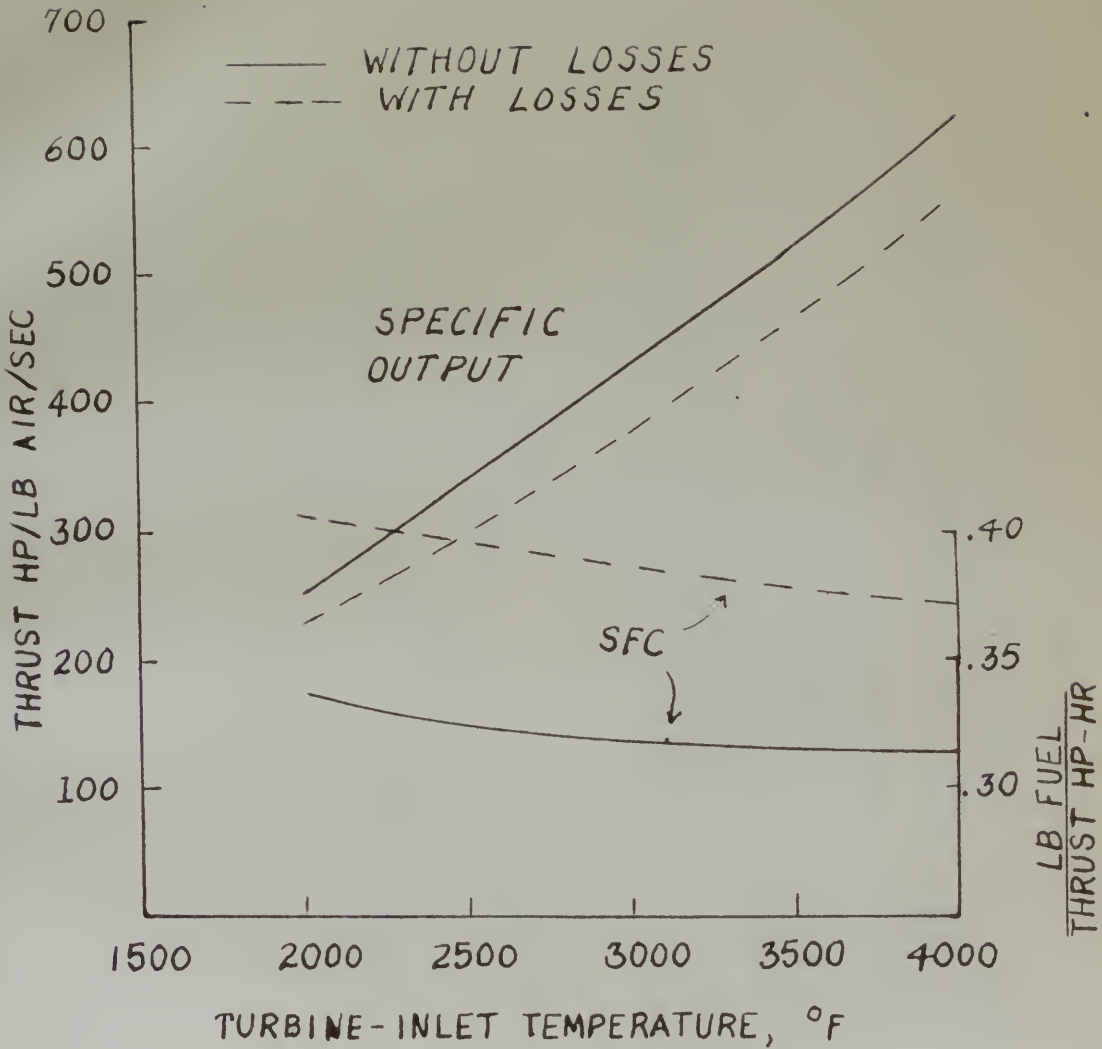
COOLING AIR DP "H ₂ O	W _a	300°F		1000°F		1200°F		1400°F		1600°F	
		TBLE T.R.	TBTE T.R.	TBLE T.R.	TBTE T.R.	TBLE T.R.	TBTE T.R.	TBLE T.R.	TBTE T.R.	TBLE T.R.	TBTE T.R.
0	0	777	785	995	1000	1175	1200	1370	1375	1535	1570
.1	.217	720	57 750 35	912	95 163 37	1052	143 1135 65	1210	120 1338 51	1470	15 1550 40
.2	.345	710	67 750 35	875	100 750 50	1042	150 1127 73	1230	160 1345 70	1422	163 1540 50
.3	.471	645	82 750 35	860	135 740 60	1035	160 1120 80	1202	188 1312 83	1388	187 1550 40
.4	.600	685	72 750 35	850	145 740 60	1015	180 1120 80	1175	215 1303 72	1365	220 1550 40
.5	.726	610	107 750 35	835	160 740 60	1010	185 1120 80	1150	240 1300 75	1340	245 1550 40
.6	.846	655	122 750 35	825	170 740 60	985	210 1120 80	1135	255 1300 75	1315	270 1540 50
.7	.972	650	127 750 35	815	180 740 60	975	220 1120 80	1120	270 1300 75		
.8	1.09	645	132 750 35	800	175 730 70	965	230 1120 80				
0	0	720	725	930	945	1142	1147	1325	1320	1470	1480
.1	.217	645	75 706 17	860	170 730 15	1042	100 1120 27	1188	137 1285 35	1385	125 1455 25
.2	.345	640	80 700 25	850	130 725 20	1030	112 1120 27	1182	143 1285 35	1365	125 1455 25
.3	.471	632	88 700 25	837	133 725 20	1015	127 1110 37	1175	150 1275 45	1336	164 1450 30
.4	.600	625	75 700 25	825	205 725 20	1000	142 1100 47	1120	205 1270 50	1275	215 1438 40
.5	.726	605	115 675 30	800	230 715 30	965	117 1075 52	1108	217 1255 67	1250	240 1425 55
.6	.846										
.7	.972										
.8	1.09										

RUN 3 CONFIGURATION A
 RUN 4 CONFIGURATION B

INSUFFICIENT COMPRESSED AIR SUPPLY

	800°F	1000°F	1200°F	1400°F	1600°F
P ₁ PSI	49	61	67	73	79
W ₁ lb/hr	47	65	80	90	103
DP _{B.A.} "H ₂ O	1.05	.75	.88	.83	.80
WB.A. lb/sec	2.16	2.06	1.78	1.72	1.87
P ₃ "H ₂ O	7.1	7.8	8.4	8.6	9.1
PT ₃ "H ₂ O	8.5	8.0	8.6	8.7	9.3
P ₄ "H ₂ O	.8	.55	.4	.32	.30
PT ₄ "H ₂ O	5.8	5.8	6.55	6.45	7.35
8 "H ₂ O	5.3	5.25	6.15	6.00	7.05
M ₁	.777	.500	.557	.545	.60

TEMPS: COOLING AIR 80°F PRESS: ATMOSPHERIC 27.82 "H₂O
 AMBIENT TEST CELL 120°F AMBIENT TEST CELL 27.50 "H₂O



TURBOPROP ENGINE PERFORMANCE WITH +WITHOUT COOLING LOSSES. AIRPLANE SPEED, 500 MPH: MACH NO., 0.69; ALTITUDE 30,000 FT. (Ref. 1)

Fig. 1

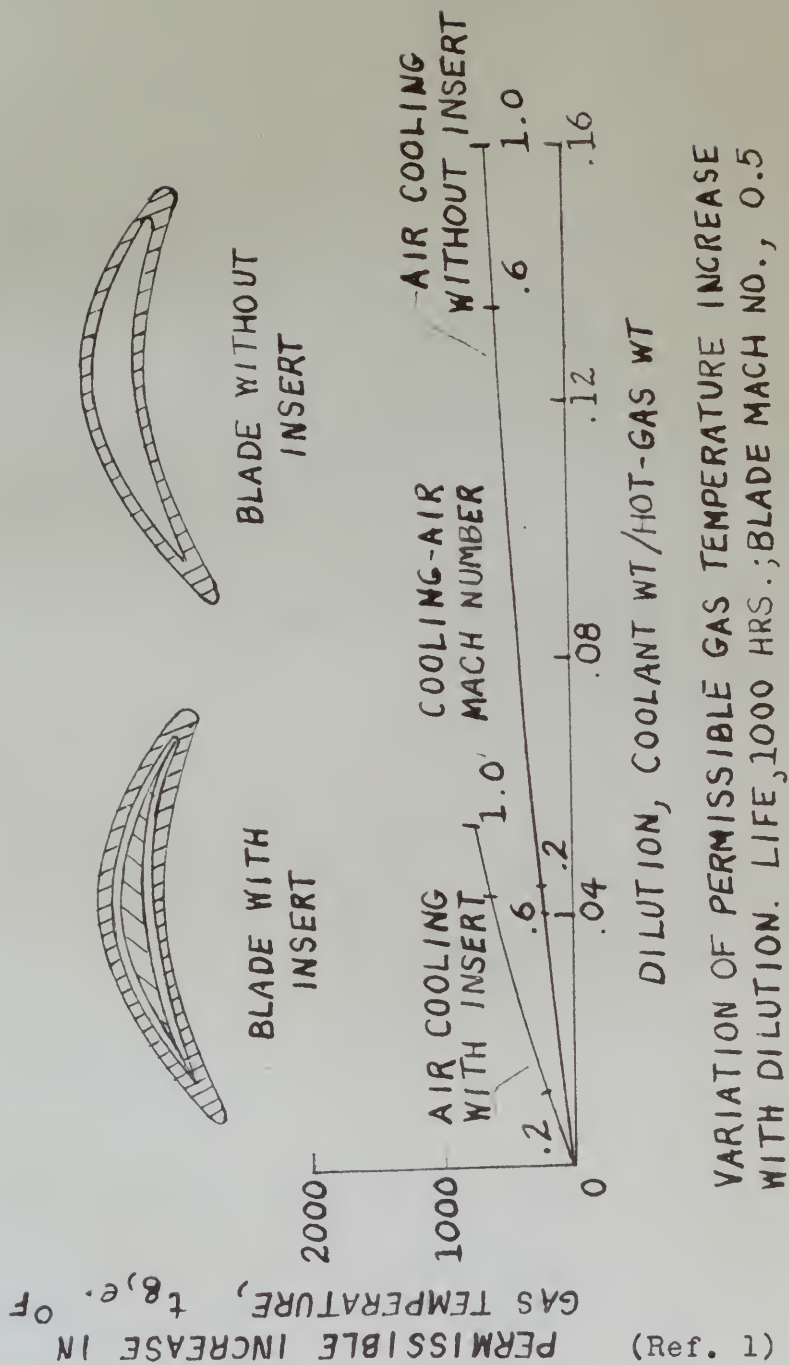
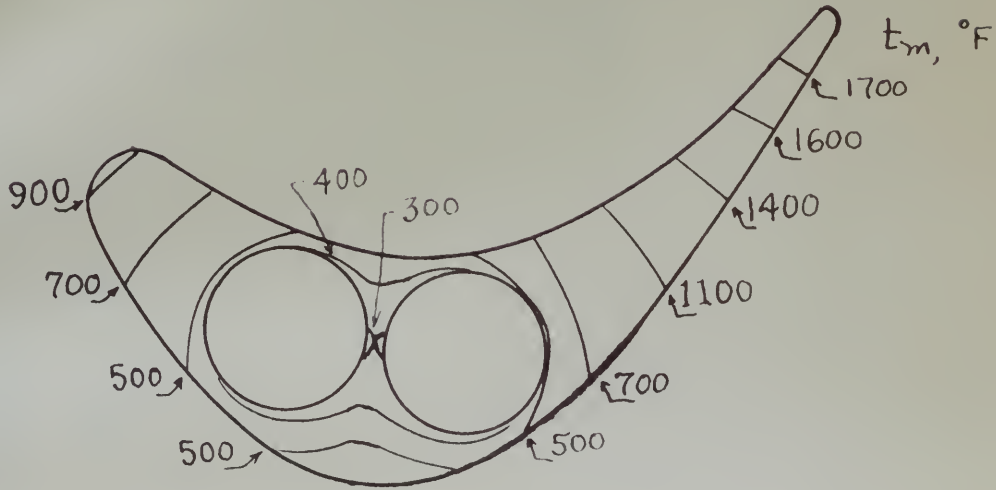
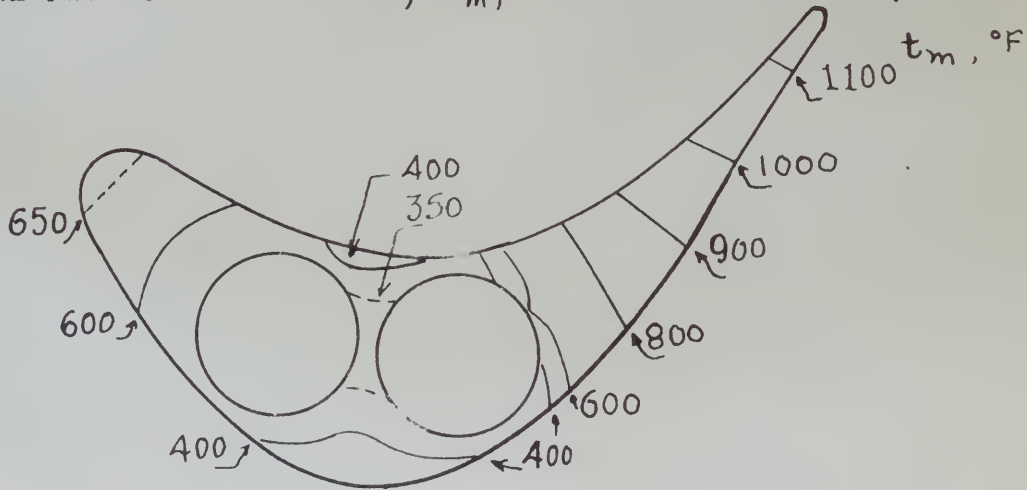


Fig. 2

THERMAL CONDUCTIVITY, k_m , 15 BTU/(HR)(°F)(FT)

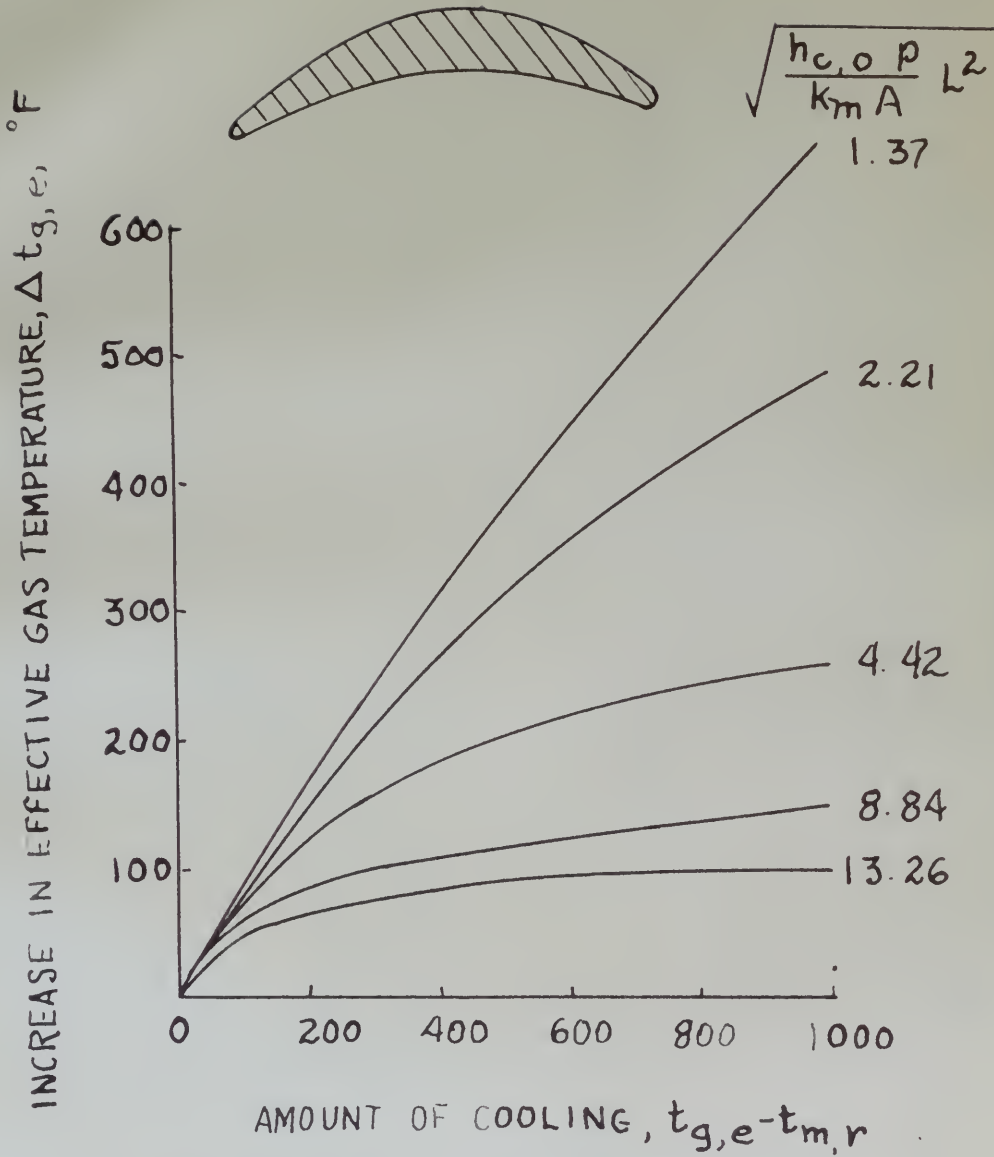


THERMAL CONDUCTIVITY, k_m , 100 BTU/(HR)(°F)(FT)



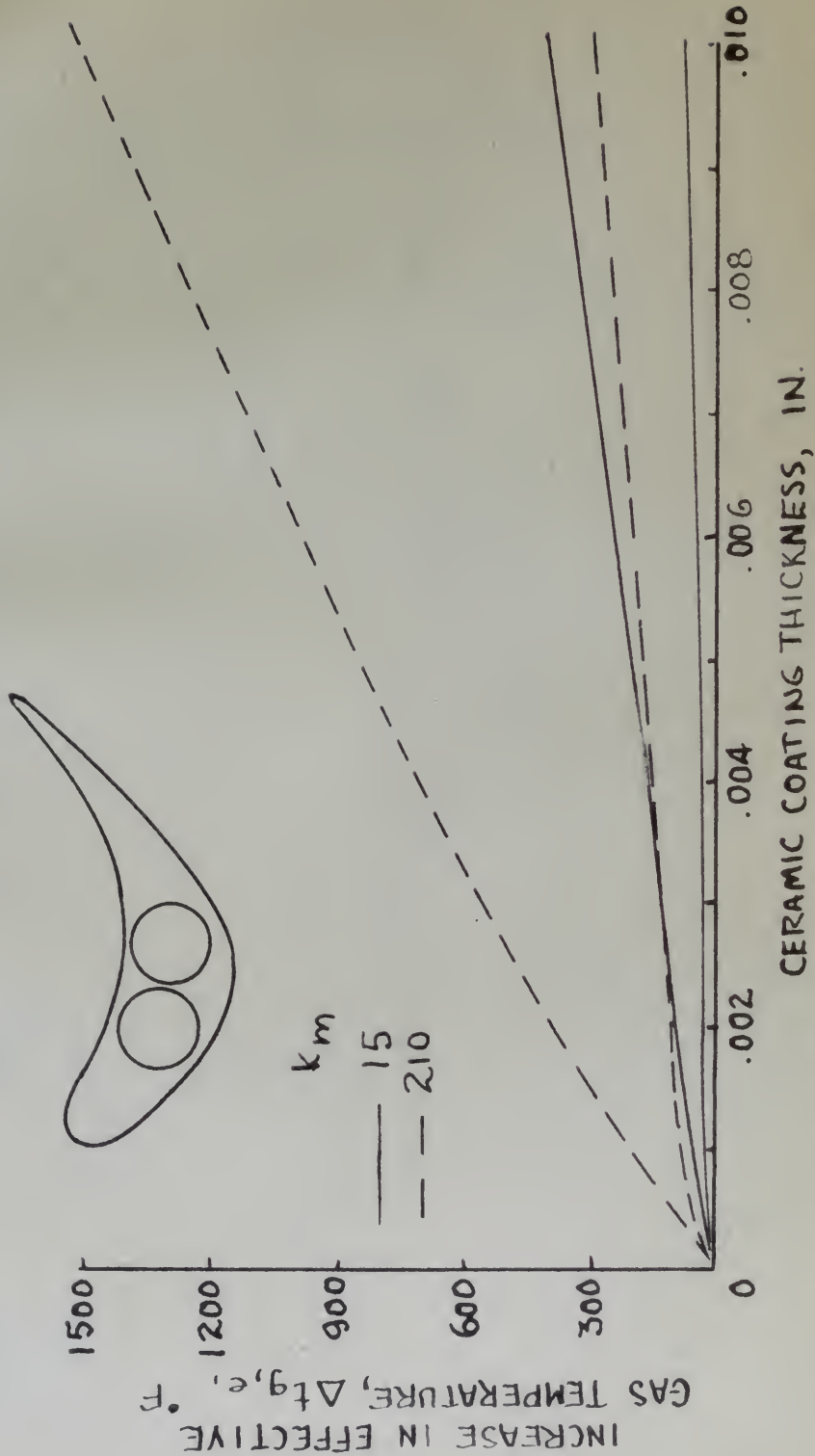
ISOTHERMS IN BLADE SECTIONS OF DIFFERENT CONDUCTIVITY MATERIAL WITH LIQUID COOLING. GAS FLOW, 55 LB/SEC; WATER FLOW, 6.42 LB/SEC; GAS TEMPERATURE, 2000° F; WATER TEMPERATURE, 200° F. (Ref. 1)

Fig. 3



VARIATION OF RIM COOLING EFFECTIVENESS.
MAXIMUM ALLOWABLE MACH NUMBER, 0.5.
(Ref. 1)

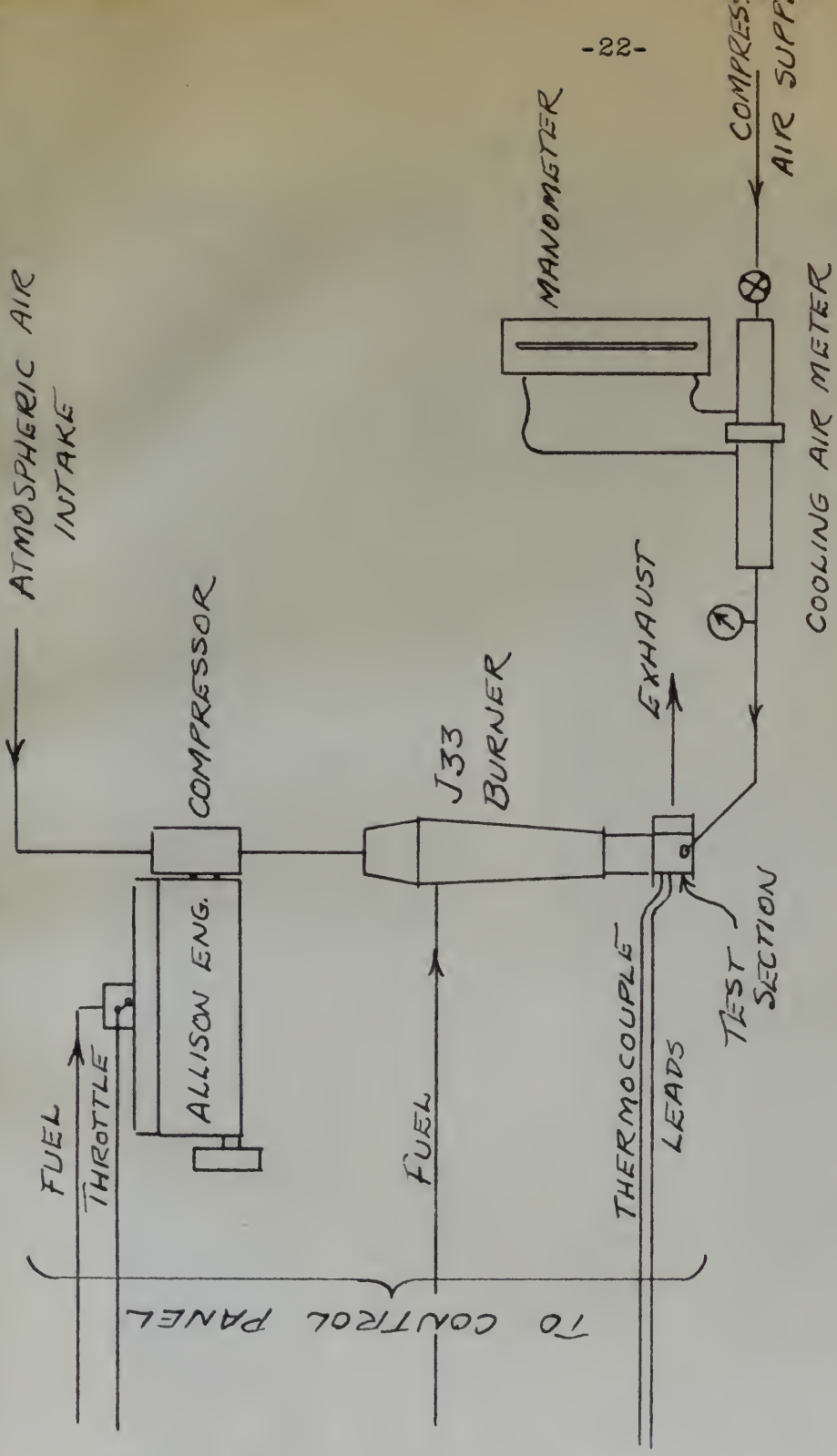
Fig. 4



VARIATION OF INCREASE IN EFFECTIVE GAS TEMPERATURE WITH CERAMIC COATING THICKNESS FOR TWO METAL AND CERAMIC THERMAL CONDUCTIVITIES.

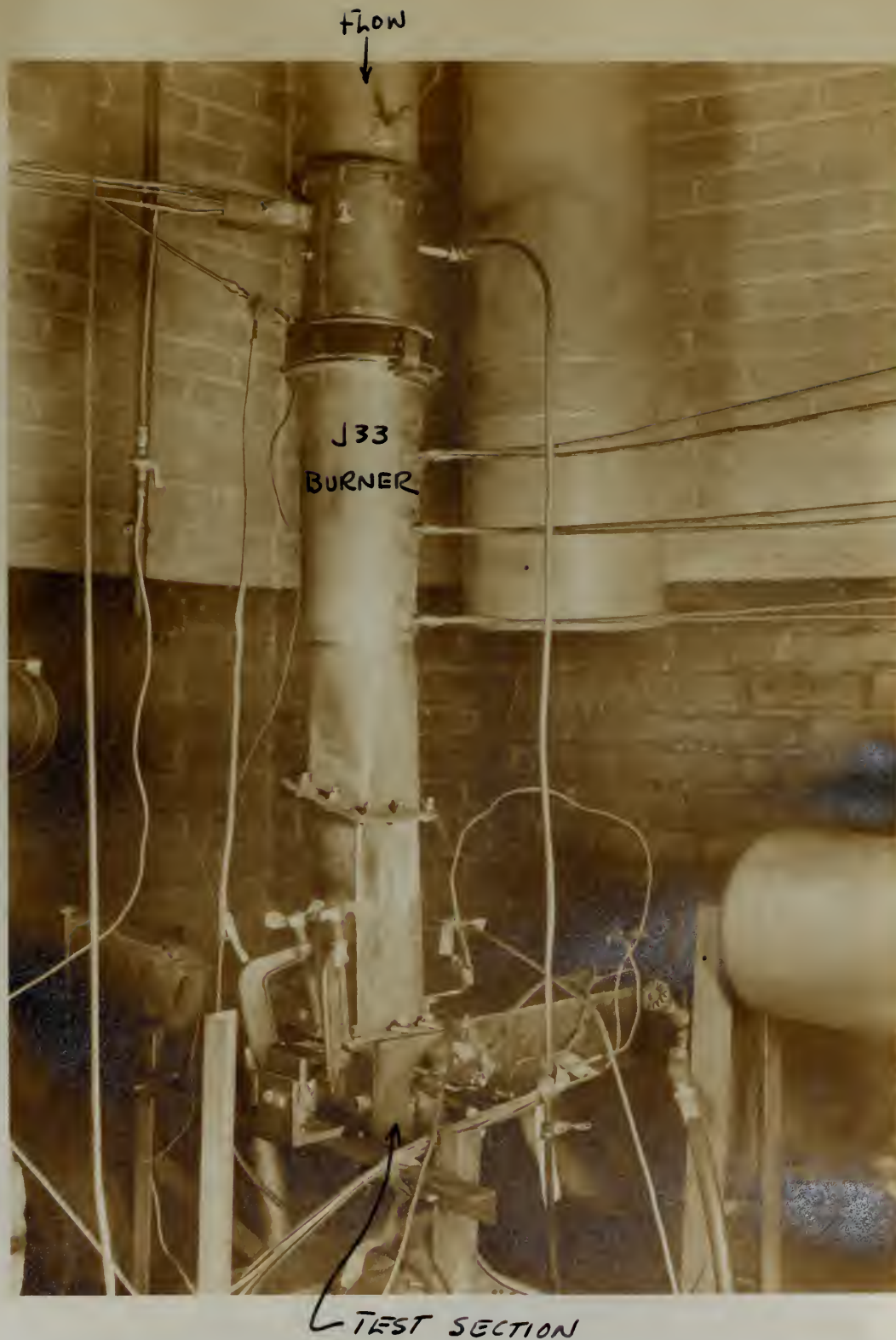
(Ref. 1)

Fig. 5



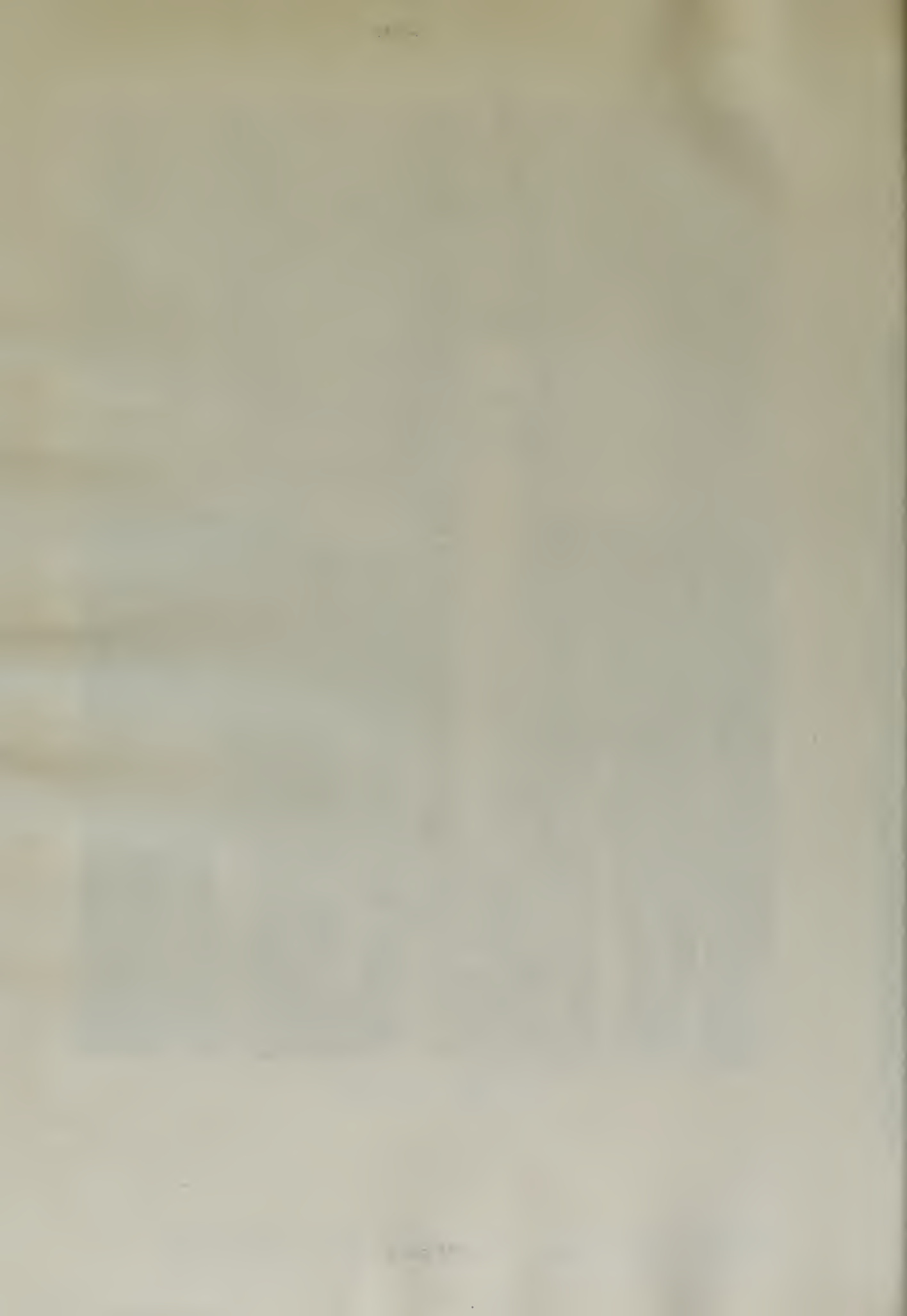
SCHEMATIC DIAGRAM OF COMPLETE TEST LAYOUT

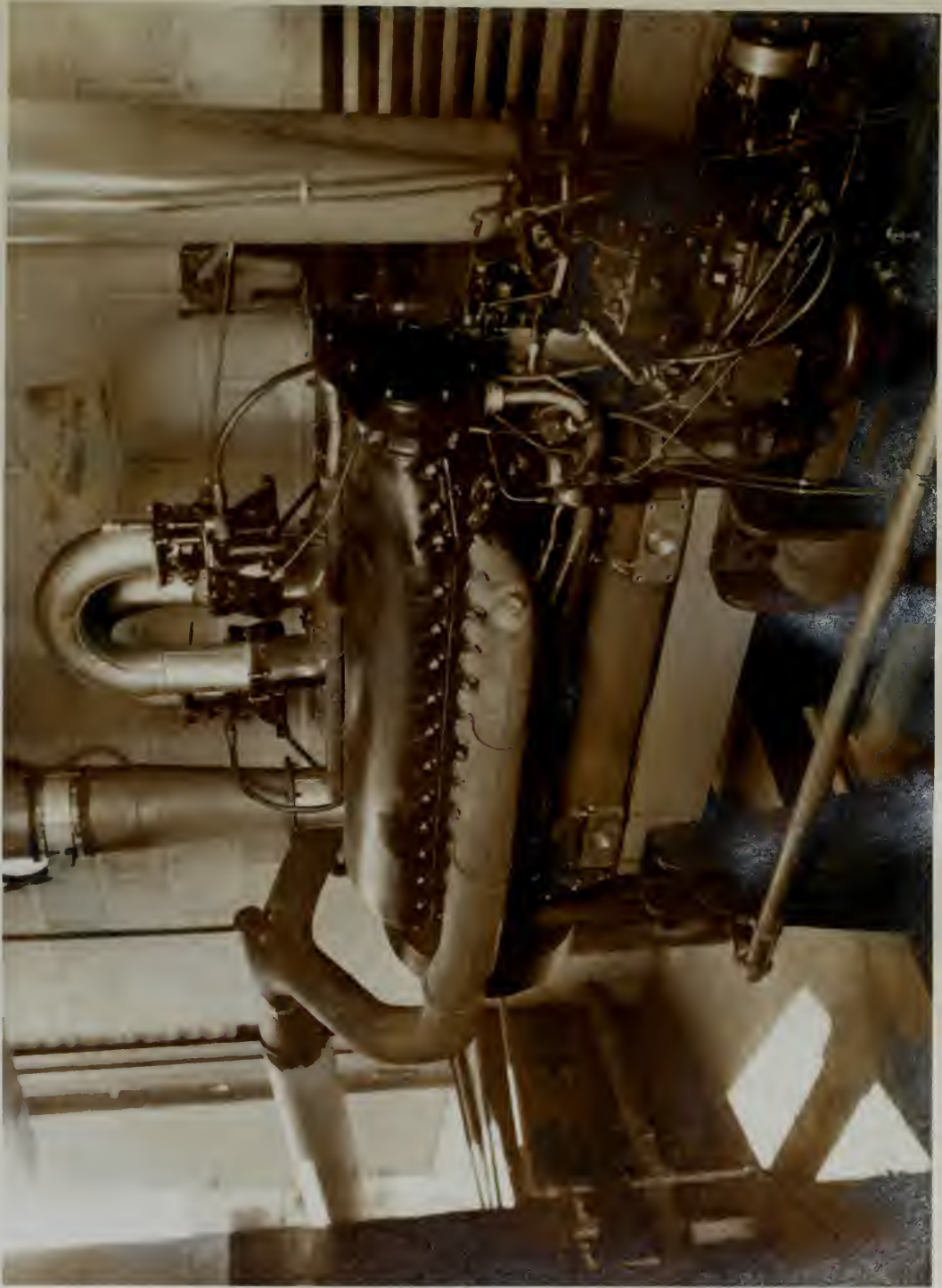
Fig. 6



TEST SECTION MOUNTED ON BURNER

Fig. 7

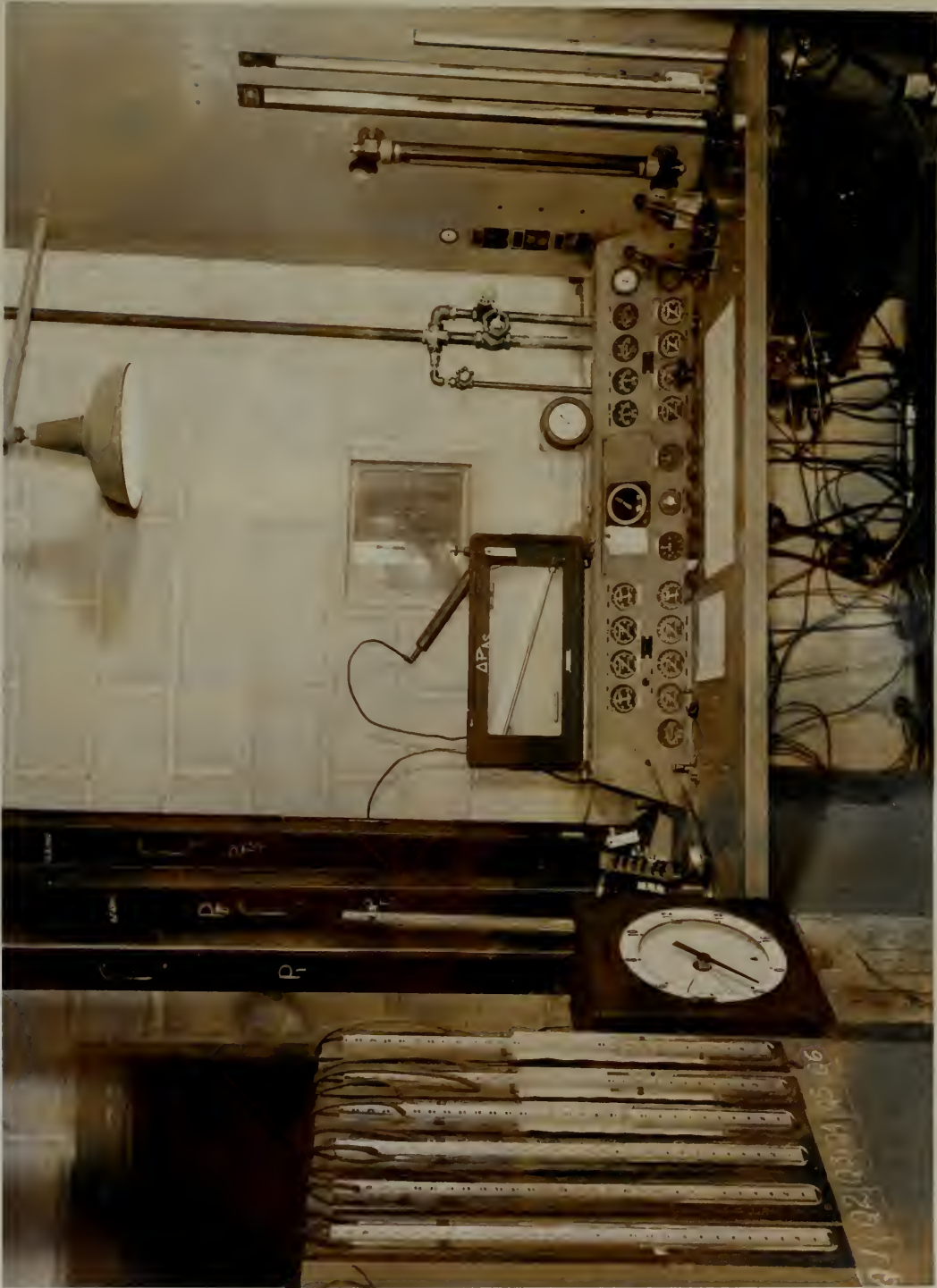




ANKISON ENGINE

Fig. 8





CONTROL PANEL

Fig. 9





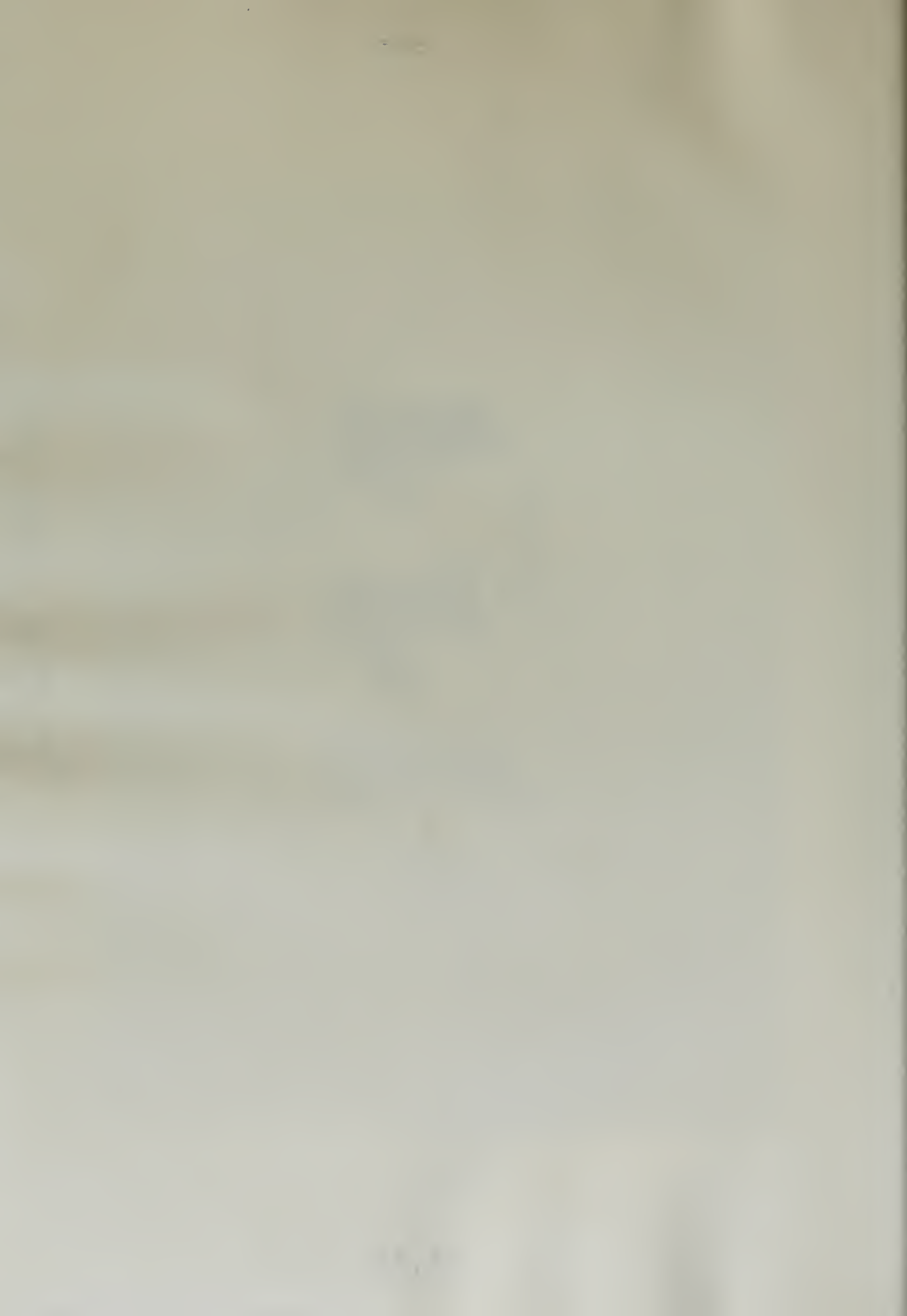
COOKING AIR METER

Fig. 10

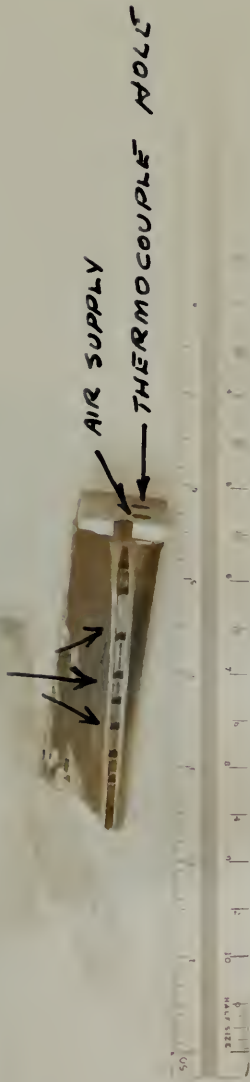




Fig. 11

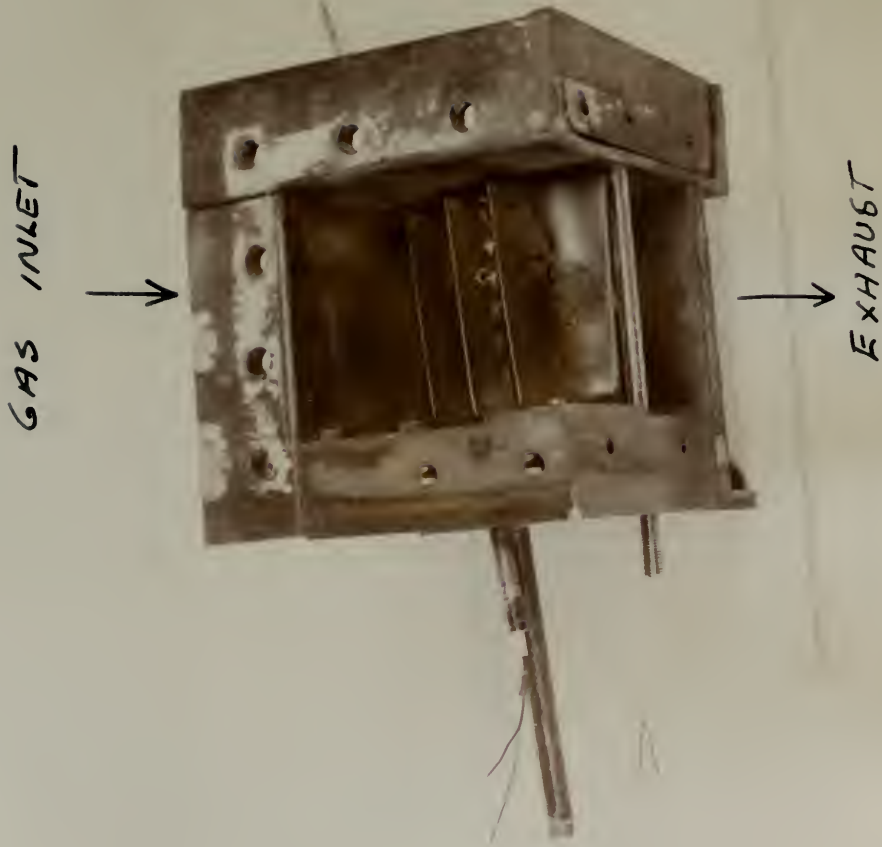


LEADING EDGE BLEEDS



TEST BLADE (CONF. B)

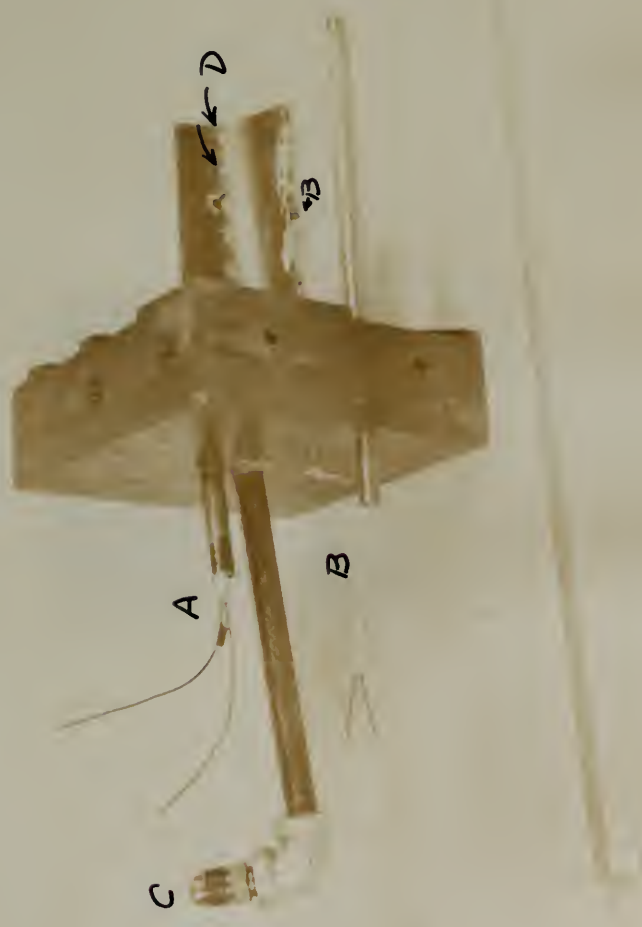
Fig. 12



COMPLETE TEST SECTION

Fig. 13

- A- LEADING EDGE
THERMOCOUPLE
- B- TRAILING EDGE
THERMOCOUPLE
- C- COOLING AIR SUPPLY
- D- " " BLEEDS



MOUNTED TEST BLADE

Fig. 14

GAS INLET



EXHAUST



END VIEW OF BLADES

Fig. 15

CONFIGURATION A

BURNER AIR FLOW - 155 to 170 lb/min

MACH NO \approx .77

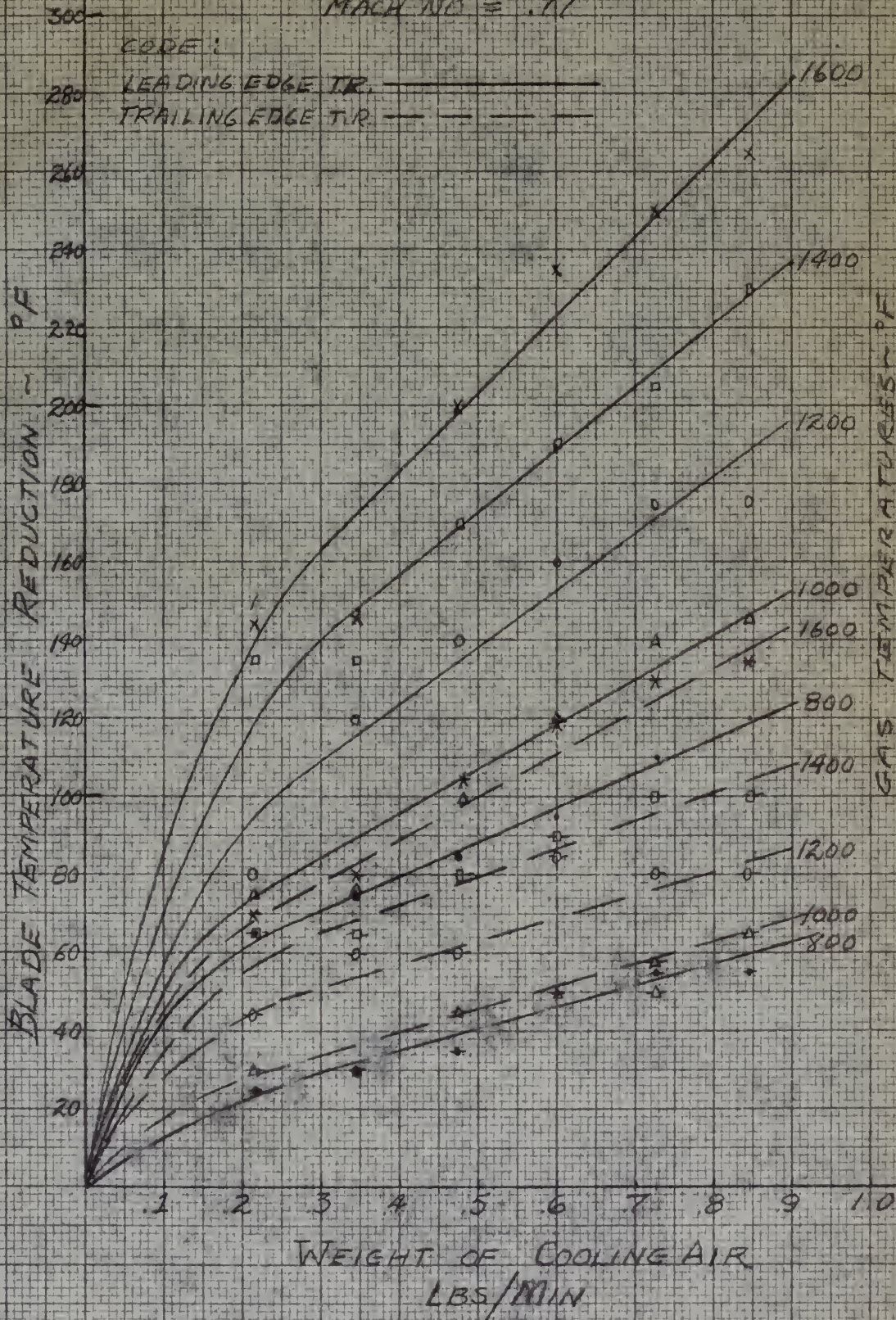
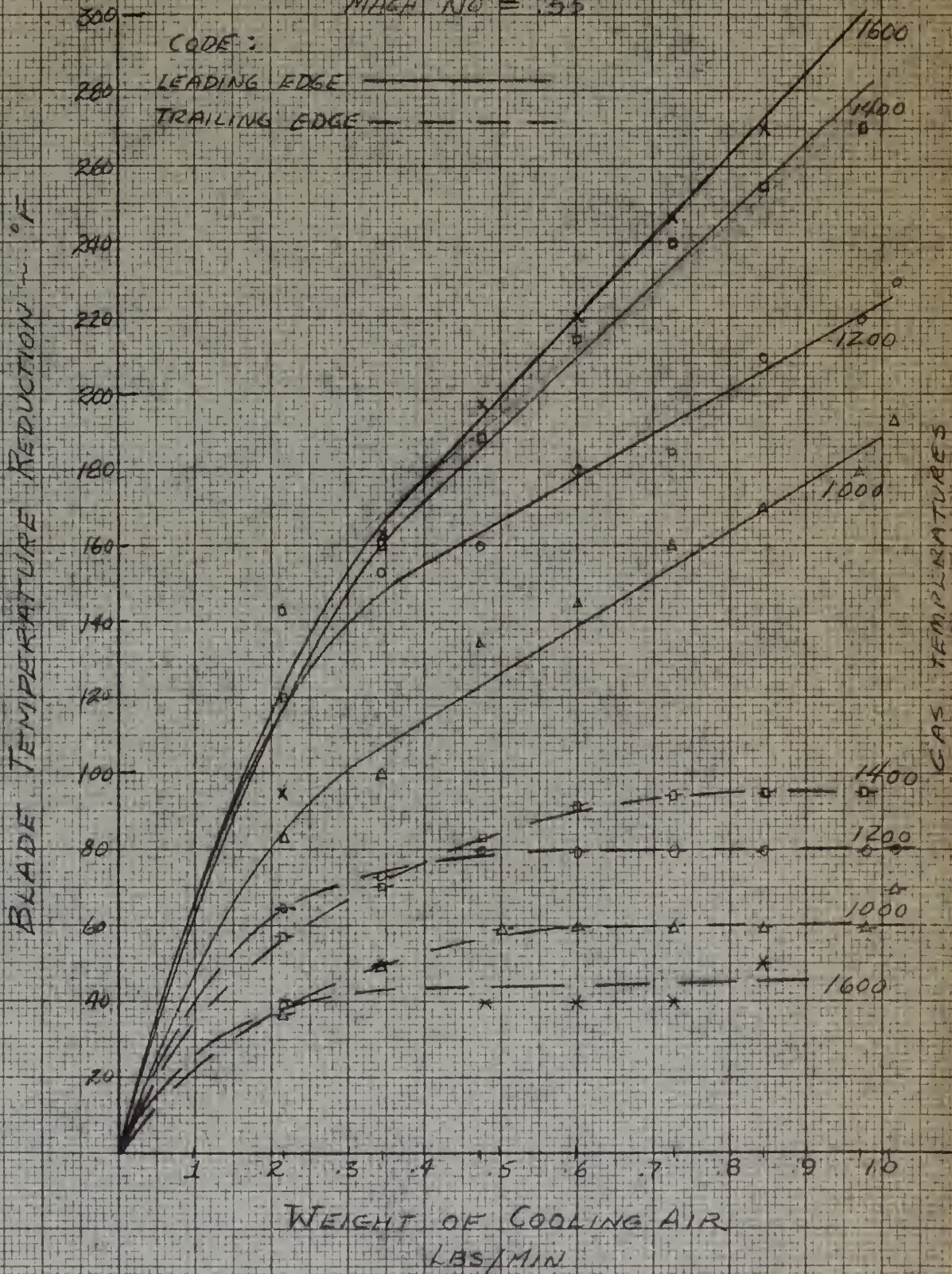


FIG 16

CONFIGURATION A
BURNER AIR FLOW - 108 to 130 lb/min
MACH NO \approx .55



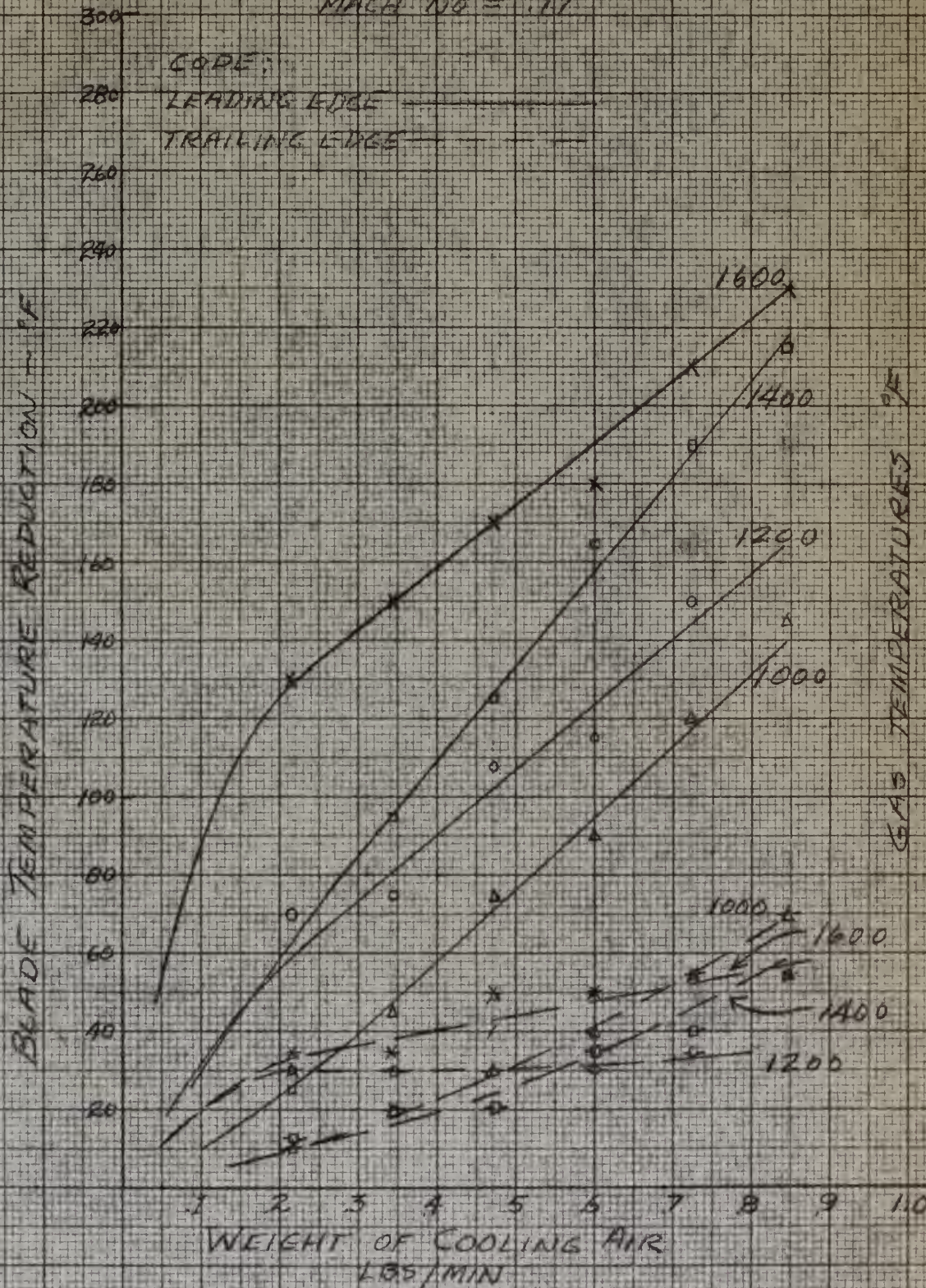
EFFECTIVENESS OF BOUNDARY LAYER
IN REDUCING BLADE TEMPERATURE



CONFIGURATION B

BURNER AIR FLOW - 155-170 lb/min.

MACH NO \approx .77



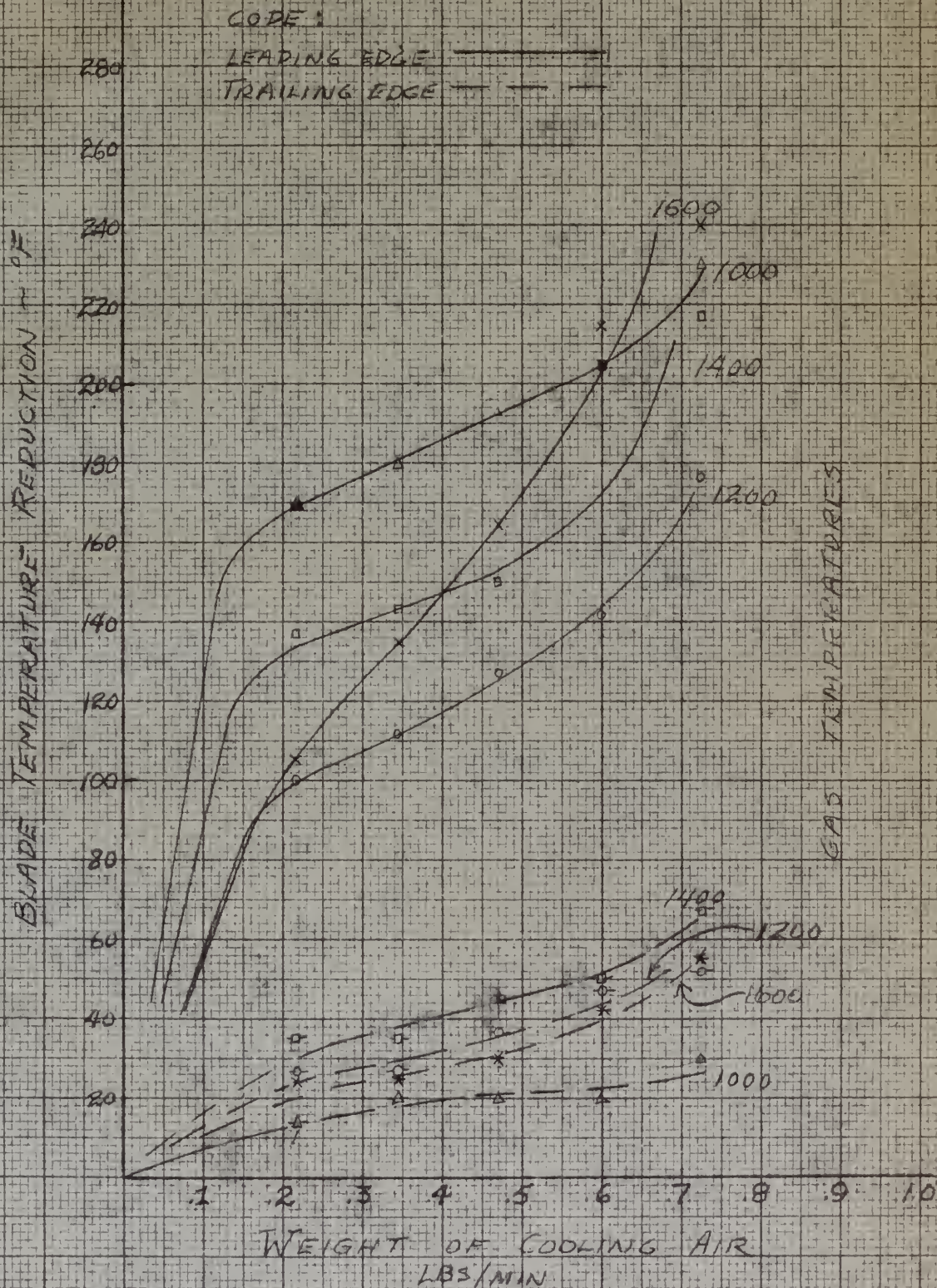
EFFECTIVENESS OF BOUNDARY LAYER
IN REDUCING BLADE TEMPERATURES

Fig. 18



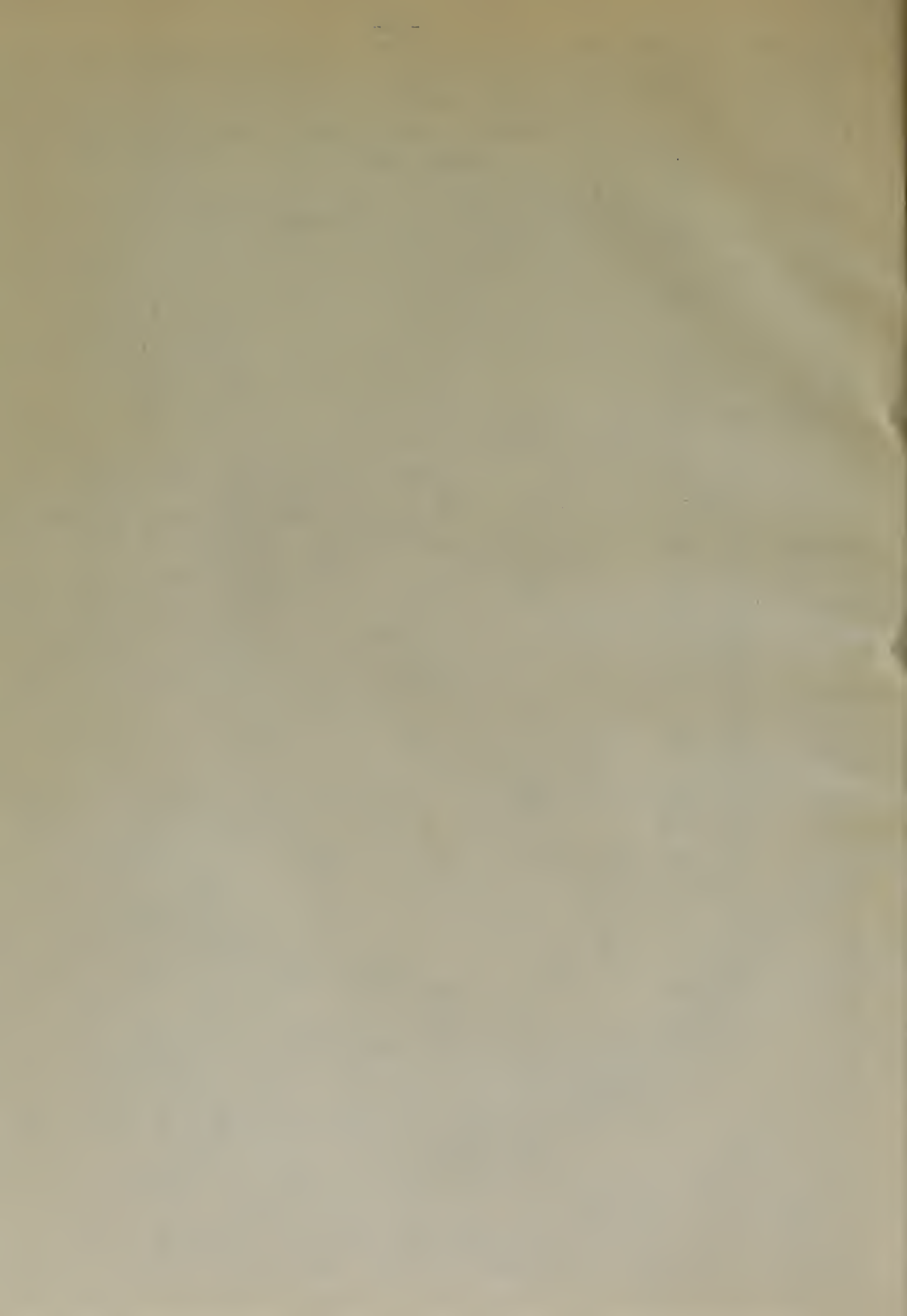
CONFIGURATION B

BURNER AIR FLOW - 108 to 130 lb/min
 MACH NO. \approx .55



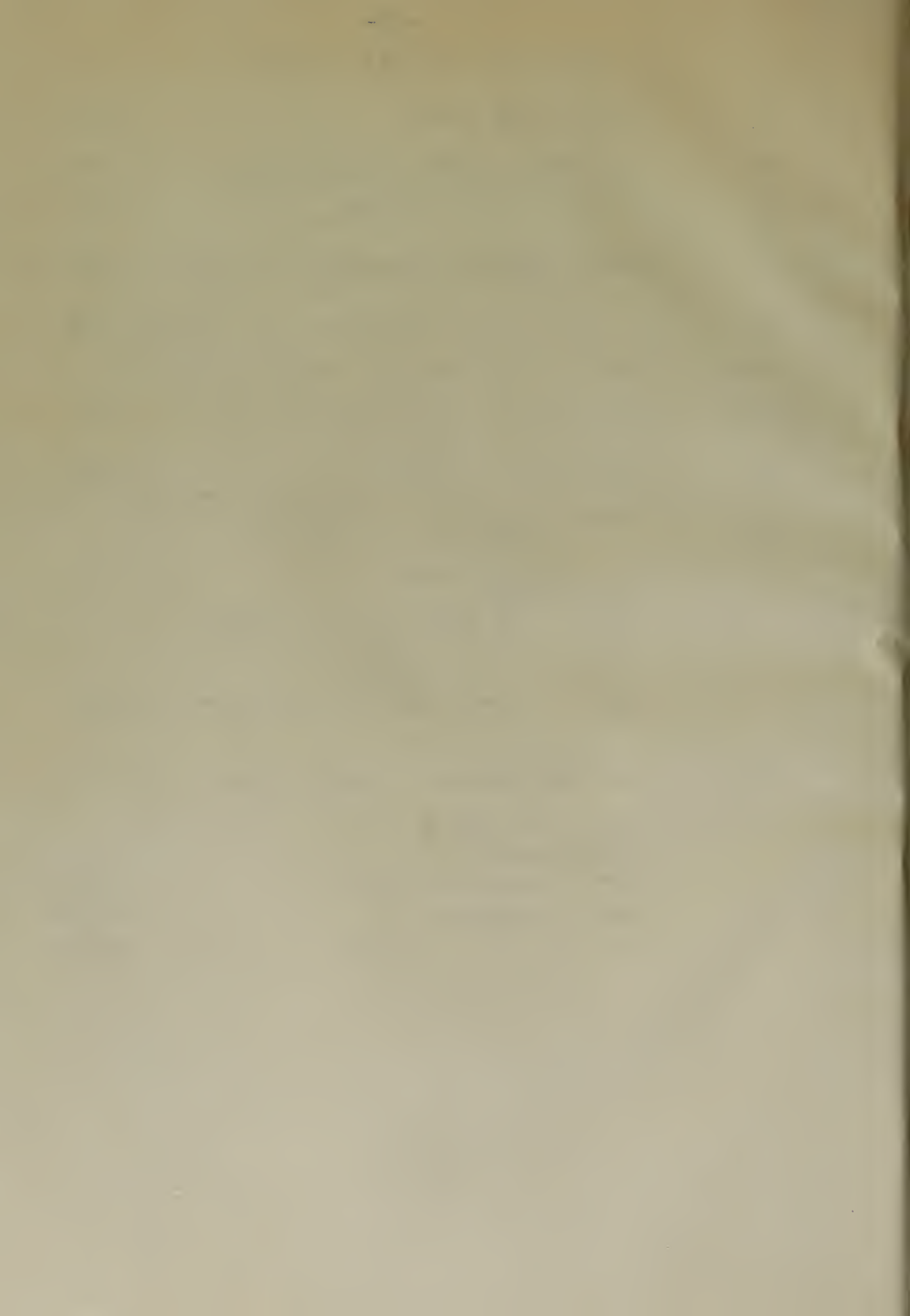
EFFECTIVENESS OF BOUNDARY LAYER
 IN REDUCING BLADE TEMPERATURES

Fig. 19



NOMENCLATURE

P_f	FUEL PRESSURE	psia
P_3	BURNER INLET STATIC PRESS	" Hg
P_{t3}	" " TOTAL "	" Hg
P_4	TEST SECTION STATIC "	" Hg
P_{t4}	" " TOTAL "	" Hg
ΔP_{CA}	COOLING AIR ORIFICE PRESS DROP	" H ₂ O
ΔP_{BA}	BURNER " " "	" Hg
f	DYNAMIC PRESS	" Hg
M_4	TEST SECTION MACH NO.	
T	TEMPERATURE	°F
	SUBSCRIPTS:	
	BLE BLADE LEADING EDGE	
	BTE " TRAILING "	
	M, R " ROOT	
	G, C GAS, AFFECTING HEAT TRANSFER	
T.R.	TEMPERATURE REDUCTION	°F
W	WEIGHT FLOW	
	SUBSCRIPTS:	
	CA COOLING AIR	lb/min
	BA BURNER "	lb/sec
	f " FUEL	lb/hr



BIBLIOGRAPHY AND REFERENCES

- (1) Ellerbrock, H. H.; "NACA Investigations of Gas Turbine Blade Cooling;" I. Ae. Sc. Reprint #117.
- (2) Smith, G. G.; "Gas Turbines and Jet Propulsion for Aircraft," 4th Ed., Aircraft Books, Inc. 1946.
- (3) Stewart, R. W.; "Literature Survey on the Use of Ceramic Materials for Turbine Blading." Allis-Chalmers Manufacturing Co., Turbopower Development Department Report, 16 March, 1948.
- (4) McAdams, W. H.; "Heat Transmission;" 2nd Ed., McGraw-Hill Book Co., 1942.

ASSIGNMENT AND REFERENCES

- (1) Winters, W. H. "The Investigation of the Victim's Mind" - J. Am. Acad. Psychiatry 1911.
- (2) Wells, G. H. "The Psychology and the Treatment of the Victim" - J. Am. Acad. Psychiatry 1911.
- (3) Wells, G. H. "The Psychology of the Victim" - J. Am. Acad. Psychiatry 1911.
- (4) Wells, G. H. "The Psychology of the Victim" - J. Am. Acad. Psychiatry 1911.

SAMPLE CALCULATIONS

Air metering: With standard sharp edged orifice configuration with flange taps.

Cooling air,

$$W_a = .8595 K D_2^2 \frac{(P_2 \cdot \Delta P)^{\frac{1}{2}}}{(T_a)^{\frac{1}{2}}} \quad (\text{ASME Power Test Code})$$

$T_a = 80^\circ \text{ F.}$ Air supply temperature

$D_2 = .75''$ Orifice diameter

$D_1 = 2.07''$ Pipe diameter

$K = .61$ From Fig. 34(a) of ASME Power Test Codes

$P_2 =$ Absolute outlet static pressure lb./in.²

$\Delta P =$ Orifice static pressure drop lb./in.²

$$W_a = \frac{.8596 \times .61 \times (.75)^2}{(540)^{\frac{1}{2}}} (P_2 \times \Delta P)^{\frac{1}{2}}$$

$$= .01268 (P_2 \times \Delta P)^{\frac{1}{2}}$$

P	P(psi)	P ₂	W _a (lb./sec.)	W _a (lb./min.)
.1	.0036	22.6	.00362	.217
.2	.0072	28.6	.00575	.345
.3	.0108	35.6	.00785	.471
.4	.0144	43.6	.01	.60
.5	.0180	50.6	.0121	.726
.6	.0216	57.6	.0141	.846
.7	.0252	64.6	.0162	.972
.8	.0288	71.6	.0182	1.09

Burner air,

$$W_{BA} = .8596 K \frac{D_2^2}{T_1^{\frac{1}{2}}} (P_2 \times \Delta P)^{\frac{1}{2}}$$

$K = .704$

$D_2 = 5.6$

Results are tabulated in Tables I and II.

SAVING CALCULATIONS

with standard sharp edged orifice
venturiometer with linear scale.

cooling air.

$$Q = \frac{C_d A \sqrt{2gh}}{14.7} \left(\frac{P_1}{P_2} \right)^{0.5} \left(\frac{P_2}{P_3} \right)^{0.5} \dots$$

at 80° F. air supply temperature

at 70° F. air supply temperature

at 60° F. air supply temperature

from fig. 2 (a) of 1933 paper
today

at 50° F. air supply temperature
today

at 40° F. air supply temperature
today

$$Q = \frac{C_d A \sqrt{2gh}}{14.7} \left(\frac{P_1}{P_2} \right)^{0.5} \left(\frac{P_2}{P_3} \right)^{0.5} \dots$$

$$Q = \frac{C_d A \sqrt{2gh}}{14.7} \left(\frac{P_1}{P_2} \right)^{0.5} \left(\frac{P_2}{P_3} \right)^{0.5} \dots$$

Pressure (psi)	Temperature (°F)	Flow (gpm)	Flow (gpm)
1.0	80	1.0	1.0
2.0	80	1.41	1.41
3.0	80	1.73	1.73
4.0	80	2.00	2.00
5.0	80	2.24	2.24
6.0	80	2.45	2.45
7.0	80	2.63	2.63
8.0	80	2.78	2.78
9.0	80	2.91	2.91
10.0	80	3.03	3.03

hotter air.

$$Q = \frac{C_d A \sqrt{2gh}}{14.7} \left(\frac{P_1}{P_2} \right)^{0.5} \left(\frac{P_2}{P_3} \right)^{0.5} \dots$$

at 70° F.
at 60° F.

Results are tabulated in Tables 1 and 2.

Mach. number:

$$q = \frac{\gamma}{2} \rho V^2$$

M_4 = Test section mach. no.

q = Test section dynamic pressure

γ = 1.3 for gas

P_4 = Test section static pressure

$$M_4 = \frac{2q}{\gamma P_4} = \frac{q}{.65 P_4}$$

Results are tabulated in Tables I and II.

Each member:

$$p = \frac{R}{1 + \frac{R}{p}}$$

$p_1 = \text{Total section mass, etc.}$

$p_2 = \text{Total section mass, etc.}$

$\gamma = 1.5 \text{ for gas}$

$p_3 = \text{Total section mass, etc.}$

$$p_4 = \frac{p_1}{1 + \frac{p_1}{p_2}}$$

Results are tabulated in Tables I and II.

Table I	Table II	Table III	Table IV	Table V
...
...
...
...
...

TABLE I
 TABLE II
 TABLE III
 TABLE IV
 TABLE V

The Thesis
N4 N4

11472

Ness

Boundary layer control
as a method of gas tur-
bine blade cooling.

Thesis
N4

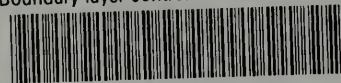
11472

Ness

Boundary layer control
as a method of gas tur-
bine blade cooling.

thesN4

Boundary layer control as a method of ga



3 2768 001 89905 7

DUDLEY KNOX LIBRARY